Progress in Biophysics and Molecular Biology 130 (2017) 198–211

Contents lists available at ScienceDirect

Progress in Biophysics and Molecular Biology

journal homepage: www.elsevier.com/locate/pbiomolbio

Original Research

Intrinsic regulation of sinoatrial node function and the zebrafish as a model of stretch effects on pacemaking

Eilidh A. MacDonald [a], Matthew R. Stoyek [a], Robert A. Rose [b], T. Alexander Quinn [a, c, *]

[a] Department of Physiology and Biophysics, Dalhousie University, Halifax, Canada
[b] Libin Cardiovascular Institute of Alberta, University of Calgary, Calgary, Alberta, Canada
[c] School of Biomedical Engineering, Dalhousie University, Halifax, Canada

ARTICLE INFO

Article history:
Received 15 February 2017
Received in revised form
17 July 2017
Accepted 21 July 2017
Available online 22 July 2017

Keywords:
Autoregulation
Heart rate
Intracardiac nervous system
Mechano-electric coupling
Natriuretic peptides
Stretch-activated channels

ABSTRACT

Excitation of the heart occurs in a specialised region known as the sinoatrial node (SAN). Tight regulation of SAN function is essential for the maintenance of normal heart rhythm and the response to (patho-) physiological changes. The SAN is regulated by extrinsic (central nervous system) and intrinsic (neurons, peptides, mechanics) factors. The positive chronotropic response to stretch in particular is essential for beat-by-beat adaptation to changes in hemodynamic load. Yet, the mechanism of this stretch response is unknown, due in part to the lack of an appropriate experimental model for targeted investigations. We have been investigating the zebrafish as a model for the study of intrinsic regulation of SAN function. In this paper, we first briefly review current knowledge of the principal components of extrinsic and intrinsic SAN regulation, derived primarily from experiments in mammals, followed by a description of the zebrafish as a novel experimental model for studies of intrinsic SAN regulation. This mini-review is followed by an original investigation of the response of the zebrafish isolated SAN to controlled stretch. Stretch causes an immediate and continuous increase in beating rate in the zebrafish isolated SAN. This increase reaches a maximum part way through a period of sustained stretch, with the total change dependent on the magnitude and direction of stretch. This is comparable to what occurs in isolated SAN from most mammals (including human), suggesting that the zebrafish is a novel experimental model for the study of mechanisms involved in the intrinsic regulation of SAN function by mechanical effects.

1. Sinoatrial node function

Excitation of the heart, which is responsible for its pumping action, begins within the organ itself - originating from specialised tissue known as the sinoatrial node (SAN). It was more than 135 years ago that Walter Gaskell first established the 'myogenic' origin of cardiac rhythm generation (Gaskell, 1882), and twenty-five years later that its anatomical location was identified (Keith and Flack, 1907). Yet, even more than a century on, mechanisms of spontaneous pacemaker activity are still debated (DiFrancesco and Noble, 2012; Maltsev and Lakatta, 2012; Rosen et al., 2012).

What is clear, derived primarily from mammalian studies, is that cardiac pacemaking involves a robust, flexible system, integrating multiple contributors that allow rapid adaptation to changes in circulatory demand (Irisawa et al., 1993). Normal automaticity requires spontaneous diastolic depolarisation (DD) of SAN cells. This involves a positive inward current ('funny' current, I_f), passing through hyperpolarization-activated cyclic nucleotide-gated (HCN) channels, acting in early diastole against reducing outward potassium (K^+) currents (DiFrancesco, 2010). As diastole progresses, depolarisation rate increases as trans-sarcolemmal calcium (Ca^{2+}) flux through $Ca_V3.1$ transient (T-type) Ca^{2+} channels ($I_{Ca,T}$) and $Ca_V1.3$ long-lasting (L-type) Ca^{2+} channels ($I_{Ca,L}$) becomes dominant (Mesirca et al., 2015). Once transmembrane potential (V_m) crosses the activation threshold of $Ca_V1.2$-mediated $I_{Ca,L}$, an action potential (AP) is initiated (Mesirca et al., 2015). As this system supports rhythmic spontaneous AP generation, it has been dubbed the 'membrane-clock' (Maltsev et al., 2006). SAN automaticity is further supported by spontaneous and triggered [by $Ca_V1.3$-mediated $I_{Ca,L}$ (Torrente et al., 2016)] Ca^{2+} release from the sarcoplasmic reticulum (SR), which results in an additional depolarising current, through the sodium (Na^+)-Ca^{2+} exchanger (I_{NCX}, with one Ca^{2+} ion removed from the cell as three Na^+ ions enter) (Lakatta et al., 2008).

* Corresponding author. Department of Physiology and Biophysics, Dalhousie University, 5850 College St, Lab 3F, Halifax, NS B3H 4R2, Canada.
E-mail address: alex.quinn@dal.ca (T.A. Quinn).

http://dx.doi.org/10.1016/j.pbiomolbio.2017.07.012
0079-6107/

Abbreviations

AP	action potential
ANP	atrial natriuretic peptide
β-AR	β-adrenergic receptors
BNP	B-type natriuretic peptide
BR	beating rate
CNP	C-type natriuretic peptide
Ca^{2+}	calcium
SAC_{NS}	cation non-selective stretch-activated channels
DD	diastolic depolarisation
ECG	electrocardiogram
I_f	'funny' current
HRV	heart rate variability
HCN	hyperpolarization-activated cyclic nucleotide-gated
ICNS	intracardiac nervous system
L-type	long-lasting
$I_{Ca,L}$	long-lasting Ca^{2+} current
NP	natriuretic peptide
NPR	natriuretic peptide receptor
K^+	potassium
SR	sarcoplasmic reticulum
SAN	sinoatrial node
Na^+	sodium
I_{NCX}	sodium-calcium exchanger current
T-type	transient
$I_{Ca,T}$	transient Ca^{2+} current
V_m	transmembrane potential

As Ca^{2+} cycling remains rhythmic even after clamping of V_m, this has been conceptualised as an independent pacemaker mechanism, and is referred to as the 'Ca^{2+}-clock' (Maltsev et al., 2006). While both of these 'clocks' have been shown to be independently sufficient for SAN automaticity, they do not operate in isolation (the Ca^{2+}-clock relies on trans-sarcolemmal ion fluxes to alter V_m; the membrane-clock includes Ca^{2+} cycling), and thus they are now considered as a coupled system (V_m/Ca^{2+}-system), whose interactions contribute to robust pacemaking even when individual mechanisms are impeded (Lakatta et al., 2010).

2. Sinoatrial node regulation

Studies in mammals have also shown that regulation of the membrane/Ca^{2+}-system by factors extrinsic (external or extracardiac) and intrinsic (internal or intracardiac) to the heart is essential for the maintenance of normal SAN function and its response to physiological and pathophysiological changes.

2.1. Extrinsic regulation

The primary extrinsic mediator of SAN activity is the central nervous system, acting through direct extracardiac sympathetic and parasympathetic innervation of intracardiac neural circuits and SAN cells (Gordan et al., 2015). Terminals of sympathetic postganglionic neurons projecting from spinal cord nuclei to SAN cells release norepinephrine, which stimulates $G\alpha_s$-coupled β-adrenergic receptors (β-AR), causing an increase in intracellular cAMP levels inside the cell. As a result, the activity of cAMP-regulated effectors, such as HCN, delayed rectifier, and L- and (possibly) T-type Ca^{2+} channels, as well as SR Ca^{2+} release are augmented, increasing the rate of DD and thus the frequency of SAN excitation and beating rate (BR) (DiFrancesco, 2006; Irisawa et al., 1993). In contrast, terminals of parasympathetic neurons projecting from brainstem vagal motor nuclei to postganglionic parasympathetic neurons within the heart (which comprise the intracardiac nervous system, ICNS, involved in intrinsic regulation – see below) release acetylcholine. This release in turn stimulates intracardiac neuronal terminals to release acetylcholine, activating $G\alpha_{i/o}$-coupled cholinergic M_2 muscarinic receptors on SAN cells, which reduces intracellular cAMP concentration, causing a decrease in depolarising currents and BR (Fischmeister et al., 2006). At the same time, Gβγ subunits also contribute to a reduction in BR by directly activating G-protein-coupled inward rectifying potassium channels, resulting in membrane hyperpolarization (DiFrancesco, 1993).

It is worth noting that the function of the SAN is also affected (albeit to a lesser degree) by peptides produced in endocrine glands (Gordan et al., 2015). Circulating epinephrine and norepinephrine (and dopamine, when converted to epinephrine or norepinephrine) released by the adrenal glands will cause an increase in BR through a similar mechanism to neurotransmitters released by sympathetic neurons.

2.2. Intrinsic regulation

Intrinsic SAN regulation is similarly governed by neuronal (ICNS) and peptidic (myogenic peptides) mechanisms, as well as mechanical factors (tissue stretch).

2.2.1. Intracardiac nervous system

The ICNS comprises a collection of efferent, afferent, and interconnecting (local circuit) neurons embedded within the myocardium, which has traditionally been viewed only as a relay station for extrinsic neural input. Work in the last two decades, however, has demonstrated that this view may be overly simplistic, given the neurochemical complexity (Leger et al., 1999; Steele and Choate, 1994), distributed nature (Armour et al., 1997; Leger et al., 1999; Pauza et al., 2000; Yuan et al., 1994), and capability for local information processing of neurons within the ICNS, as well as interactions not fully explained by this traditional understanding (Armour, 2008; Rajendran et al., 2016). It is now known that the ICNS contains parasympathetic, sympathetic, and non-noradrenergic, non-cholinergic transmitters and modulators, so along with being a target of extrinsic neurons, it may also form intracardiac circuits important for the internal processing and integration of extrinsic inputs and for intracardiac reflex control of cardiac function (Ardell and Armour, 2016).

Functional and anatomical data have shown that intracardiac neurons receive inputs from extrinsic efferent parasympathetic preganglionic and sympathetic postganglionic neurons, local interneurons, and afferent neurons from other locations within the heart (Gagliardi et al., 1988; Smith, 1999). As a result, even after acute (Gagliardi et al., 1988) and chronic (Smith et al., 2001) isolation of the heart from the central nervous system (decentralisation), the ICNS remains responsive to changes in the cardiac environment. In addition, by simultaneous recordings of parasympathetic (vagal) and sympathetic (cardiopulmonary) nerves, it has been demonstrated that they can be co-activated (Koizumi et al., 1982; Kollai and Koizumi, 1979), and that adrenergic-cholinergic interactions augment activity of the ICNS in a manner that does not occur in the presence of only one input (Smith, 1999). This may be less surprising when one considers that it appears as though less than 20% of intracardiac neurons receive direct inputs from extrinsic nerves, and instead are acting as interconnecting

neurons (Armour, 2008).

While it is now appreciated that the ICNS plays an important role in the intracardiac integration of autonomic inputs and possibly in local reflex regulation of cardiac function, details of the anatomical and functional distribution and connectivity of neurons within the ICNS, and an understanding of its mechanisms of action, are incomplete. In mammals, intracardiac neurons are widely distributed in ganglia throughout both atria (Armour et al., 1997; Leger et al., 1999; Pauza et al., 2000; Steele and Choate, 1994; Steele et al., 1996), yet the projection patterns of subpopulations of intracardiac neurons to specific targets remain unknown [except to some degree in hearts of rat (Pardini et al., 1987) and guinea pig (Steele and Choate, 1994)]. This is complicated by the large number of neurons involved; in the human heart the ICNS encompasses more than 10^6 neurons (Pauza et al., 2000), in the dog heart more than 10^5 neurons (Armour and Ardell, 2004), and even in the heart of smaller animals, such as that of the guinea pig, ~2000 neurons (Leger et al., 1999). An additional difficulty stems from the fact that in mammals the ICNS is deeply embedded in, and distributed throughout, the myocardium, and thus largely inaccessible for integrative studies. One solution to this problem is the use of reduced experimental preparations representing a subset of the ICNS, such as isolated tissue, to study the properties of control circuits *in vitro* (Ardell et al., 2014; Smith, 1999). This approach, however, eliminates intracardiac neuronal connections, so allows only limited conclusions to be drawn regarding the role of localized circuitry in controlling overall cardiac function. Studies using alternative (non-mammalian) experimental models, such as the zebrafish, may provide a solution to this problem, as described below.

2.2.2. Myogenic peptides

Release of peptides contained in cardiac myocytes, fibroblasts, and endothelial cells within or in close proximity to the SAN can act in a paracrine (or autocrine) fashion to modulate SAN function. The primary factors released by cells in the atria are natriuretic peptides (NPs), a family of hormones with a number of potent effects in the cardiovascular system (Kuhn, 2004; Potter et al., 2006). Several members of the NP family of have been identified, including atrial NP (ANP), B-type NP (BNP) and C-type NP (CNP). Each of these peptides is expressed (albeit to different extents) in the heart and are present in both cardiomyocytes and cardiac fibroblasts (Moghtadaei et al., 2016).

Three NP receptors (NPR), called NPR-A, NPR-B and NPR-C, are responsible for mediating the effects of NPs upon receptor binding and activation (Potter et al., 2006). NPR-A (which binds ANP and BNP) and NPR-B (which is selectively activated by CNP) are guanylyl cyclase linked receptors that enhance cGMP signalling (Lucas et al., 2000). NPR-C (which binds all NPs with similar affinity) is coupled to inhibitory G-proteins that inhibit adenylyl cyclase (and thus cAMP) signalling (Anand-Srivastava, 2005; Rose and Giles, 2008).

NPs are best known for their capacity to regulate blood pressure and cardiovascular homeostasis as a result of their ability to induce natriuresis, diuresis, and vasodilation and to modulate endothelial permeability (Kuhn, 2004; Potter et al., 2006). Yet, NPs have recently emerged as potent regulators of cardiac electrophysiology and ion channel function (Perrin and Gollob, 2012), and have been implicated as potential contributors to arrhythmogenesis (Egom et al., 2015; Moghtadaei et al., 2016), including inherited (due to mutation of the ANP gene) atrial fibrillation in humans (Abraham et al., 2010; Hodgson-Zingman et al., 2008; Hua et al., 2015).

In the SAN, NPs can potently regulate BR through direct effects on SAN cells (Azer et al., 2012; Rose et al., 2007; Springer et al., 2012). In isolated SAN myocytes, BNP and CNP each increase BR in association with increases in the rate of DD, but without differences in maximum diastolic V_m (the effects on BR also occur in isolated hearts). Voltage clamp studies have demonstrated that the changes in BR with BNP or CNP administration result from increases in I_f and total $I_{Ca,L}$, along with shifts in the voltage dependence of channel activation. In NPR-C knockout mice, the stimulatory effects of BNP and CNP on BR, I_f, and $I_{Ca,L}$ are indistinguishable from wildtype mice in basal conditions. In contrast, the effects of BNP and CNP were reduced by the PDE3 inhibition, and the effects of BNP were antagonized by NPR-A blockade, illustrating that BNP and CNP increase SAN BR by activating the guanylyl cyclase-linked NPR-A and NPR-B receptors and inhibiting PDE3 activity (Springer et al., 2012). Consistent with these findings, ANP has also been shown to elicit a cGMP-dependent increase in I_f in human atrial myocytes (Lonardo et al., 2004).

Although NPR-C does not affect SAN function in basal conditions, it does have effects in the presence of β-AR activation (Azer et al., 2012; Springer et al., 2012). Specifically, in the presence of isoproterentol, the ring-deleted ANP analogue cANF (which only activates NPR-C) dose-dependently decreases BR by decreasing the rate of DD, effects that are absent in NPR-C knockout mice (Azer et al., 2012). In contrast, BNP and CNP (which activate NPR-A/B along with NPR-C) increases BR in the presence of submaximal doses of isoproterenol (10 nM), although effects are smaller than in basal conditions due to competing effects of NPR-A/B (increasing BR) and NPR-C (decreasing BR) stimulation. In fact, in the presence of larger doses of isoproterenol (1 μM), BNP and CNP instead decrease BR. In agreement with this observation, CNP and cANF can also decrease $I_{Ca,L}$ in SAN myocytes in the presence of high doses of isoproterenol (Rose et al., 2004). Collectively, these studies demonstrate that NPs can modulate SAN function *via* NPR-A/B receptors (stimulatory) and NPR-C (inhibitory) and that these receptors elicit opposing effects. Because of this, NPs increase BR in some conditions, but decrease BR in others, which is dependent on the extent of β-AR activation and the relative contribution of each NPR in varying physiological conditions (Azer et al., 2012, 2014; Moghtadaei et al., 2016).

While much of the focus regarding peptidic SAN regulation has been placed on the effect of NPs, BR may also be affected by a host of other locally released factors (Beaulieu and Lambert, 1998). For instance, angiotensin II, which is locally synthesised by the cardiac renin-angiotensin system and is highly concentrated at the level of the SAN artery (Saito et al., 1987), has been shown to affect BR in isolated SAN cells (Sheng et al., 2011), atrial preparations (Kobayashi et al., 1978), and intact animals (Lambert et al., 1991) *via* type 1 angiotensin II receptors (At_1) (Lambert, 1995). Similarly, endothelin-1 (as well as -3), produced and secreted by endothelial cells and acting through ET_A receptors, alters BR of isolated SAN cells (Ono et al., 2001; Tanaka et al., 1997) and atrial preparations (Ishikawa et al., 1988; Ju et al., 2011; Saito et al., 1987), in a concentration and species dependent manner.

2.2.3. Tissue stretch

Throughout the heart, function is intrinsically regulated by feedback from the myocardium's mechanical state to its electrical activity (mechano-electric feedback or coupling) (Quinn and Kohl, 2016; Quinn et al., 2014). This intracardiac phenomenon is essential for adaptation to constantly changing physiological conditions, and is important for both normal heart function (Quinn, 2015) and as a contributor to arrhythmias in various cardiac diseases (Quinn, 2014; Quinn and Kohl, 2011a).

The SAN specifically responds on a beat-by-beat basis to changes in hemodynamic load (Quinn et al., 2011a; Quinn and Kohl, 2012). First recognised in 1915 by Francis Bainbridge as an increase in BR with atrial distension by intravenous fluid injection in anaesthetised dogs (Bainbridge, 1915), similar effects have since

been observed in a wide variety of vertebrates (Pathak, 1973), including human (Donald and Shepherd, 1978). Stretch-induced increases in BR occur also in the isolated (decentralised) heart (Blinks, 1956), SAN tissue (Blinks, 1956; Deck, 1964), and SAN cells (Cooper et al., 2000), and are insensitive to ablation of intracardiac neurons (Wilson and Bolter, 2002), block of neuronal sodium channels (Chiba, 1977; Wilson and Bolter, 2002), and adrenergic and cholinergic blockade (Blinks, 1956; Brooks et al., 1966; Chiba, 1977; Wilson and Bolter, 2002), indicating that non-neuronal, intracardiac mechanisms must be involved.

Microelectrode recordings in SAN tissue have demonstrated that stretch increases maximum diastolic and decreases maximum systolic V_m, and increases DD rate (Deck, 1964). Patch-clamp recordings in axially stretched isolated SAN cells, combined with computational modelling, have demonstrated that stretch responses can be explained by a mechano-sensitive whole-cell current with a reversal potential of −11 mV (Cooper et al., 2000), presumably carried by cation non-selective stretch-activated channels (SAC_{NS}). While the molecular identity of SAC_{NS} is still not known (Peyronnet et al., 2016), it is clear that they are rapidly-activating, with a reversal potential of 0 to −20 mV in cardiac cells (Craelius et al., 1988; Guharay and Sachs, 1984), and that their block causes a reversible reduction of stretch-induced changes in BR (Cooper and Kohl, 2005). Interestingly, even if located outside of SAN cells in electrically-coupled fibroblasts (Quinn et al., 2016), SAC_{NS} can account for stretch-effects (Kohl et al., 1994), as fibroblasts possess SAC_{NS} (Stockbridge and French, 1988), are coupled to SAN cells (Camelliti et al., 2004), and are depolarised by stretch (Kohl et al., 1994; Kohl and Noble, 1996).

Of course quantitative plausibility is no substitute for validation (Quinn and Kohl, 2011b), and stretch responses may also result from direct effects on mechano-sensitive components of the V_m/Ca^{2+}-system. When expressed in oocytes, activation and deactivation rate of HCN channels are increased by mechanical stimulation (Lin et al., 2007), along with current amplitude (Calloe et al., 2005). Similarly, L-type Ca^{2+} ($Ca_V1.2$) (Calabrese et al., 2002; Lyford et al., 2002) and K^+ (Kv1, Kv3, Kv7, KvCa) (Morris, 2011) channels have been shown to be mechanically-modulated in expression systems. Furthermore, axial stretch of ventricular myocytes causes an acute increase in the frequency of spontaneous Ca^{2+} release events from the SR (Ca^{2+} sparks) *via* augmented ryanodine receptor open probability (Gamble et al., 1992; Iribe and Kohl, 2008; Iribe et al., 2009; Prosser et al., 2011, 2013). This increase in Ca^{2+} sparks may partly involve mechanically-induced mitochondrial Ca^{2+} release through the mitochondrial Na^+-Ca^{2+} exchanger (Belmonte and Morad, 2008), a channel that has been shown to alter BR in isolated SAN cells by altering Ca^{2+} spark frequency (Yaniv et al., 2012). Thus, if any of the above effects occurs also in SAN cells, they may too contribute to stretch-induced changes in BR.

There is also evidence supporting an interaction between mechanical and autonomic BR modulation. In intact animals (Bolter, 1994; Bolter and Wilson, 1999) and isolated atria (Barrett et al., 1998; Bolter, 1996; Wilson and Bolter, 2001), an increase in atrial pressure induces both BR acceleration and a significant reduction in the percentage response to vagal stimulation. *Vice versa*, when BR is reduced by vagal stimulation the stretch-induced BR response is augmented, an interaction that may be mediated by muscarinic K^+ channels, as they have been shown to close with atrial distension (Han et al., 2010). In this way, parasympathetic control of BR may be continuously modified by atrial loading, further contributing to the stretch-induced adjustment of BR to fluctuations in hemodynamic demand, helping prevent excessive slowing and diastolic distension, while maintaining cardiac output and adequate circulation (Brooks and Lange, 1977).

Response of the SAN to stretch, however, differs in some species. While in most medium and large mammals the SAN responds to stretch with an increase in BR, in mouse there is instead a decrease in BR with stretch (Cooper and Kohl, 2005). Thus, the mouse may not represent an appropriate species for the investigation of stretch-induced changes in SAN BR, which, as the primary genetically modifiable experimental model available, has hindered definition of the (still unknown) mechanisms responsible for SAN stretch responses. As for integrative studies of the ICNS, the zebrafish may represent an alternative model to address current limitations of mammalian models.

3. Zebrafish as an alternative model for cardiac electrophysiological studies

The zebrafish is becoming an increasingly powerful experimental model for the study of cardiac electrophysiological mechanisms, as: (i) it has striking similarities to human, both genetically (almost every cardiac gene has been identified to have a human ortholog with analogous function) and functionally (comparable heart rate, AP morphology, and ion channel and Ca^{2+}-handling protein expression and function); (ii) its genome has been fully sequenced and can be easily manipulated by standard techniques; and (iii) its cardiac function can be observed *in vivo* [relevant studies demonstrating these important aspects are reviewed in (Brette et al., 2008; Genge et al., 2016; Gut et al., 2017; Liu et al., 2016; Nemtsas et al., 2010; Poon and Brand, 2013; Vornanen and Hassinen, 2016)].

3.1. Advantages of the zebrafish for the study of SAN function

In regards to the utility of zebrafish for the study of SAN function, it has been shown that pacemaker activity is clearly present, functions similarly (at least in some important respects) to mammals, and is found in a ring-like structure at the location of the sinoatrial valve (the border between the sinus venosus and the atrium) (Arrenberg et al., 2010; Stoyek et al., 2015, 2016; Tessadori et al., 2012). The first indication of the currents involved in generating SAN automaticity in the zebrafish came from the discovery of a mutation (*slow mo*) that caused a reduction in heart rate by affecting a hyperpolarization-activated inward current with the properties of I_f (Baker et al., 1997; Warren et al., 2001), suggesting that the zebrafish SAN may employ similar pacemaking mechanisms to mammals. It has since been shown that SAN development in the zebrafish has similarities to mammals, occurring from *Isl1*- and *tbx2b*-expressing cells (Tessadori et al., 2012) under the control of *shox2* (Blaschke et al., 2007; Hoffmann et al., 2013), with a dependence on *Popdc1-3* (Schindler et al., 2012) and *Fhf2a* (Poon et al., 2016).

Recently, the zebrafish has been used to overcome limitations of larger animal models to explore both extrinsic autonomic, and intrinsic ICNS, regulation of the SAN (Stoyek et al., 2016). Although the relatively small size of the zebrafish heart presents its own technical challenges, it permits visualisation of, and accessibility to, the entire ICNS and its external inputs in the whole, intact organ. Specifically, it has been shown that approximately 90% of all intracardiac neurons (mean total = 197 ± 23) present in the zebrafish heart are located within the SAN region. This neuronal plexus is innervated by extrinsic axons from the left and right vagal nerves, with terminals concentrated near intracardiac ganglia, adjacent to cells expressing HCN4 (the principal HCN isoform contributing to DD in zebrafish and mammals). As would be predicted by the traditional view of the ICNS, it was found that the vast majority of intracardiac neurons in the SAN region are cholinergic; however some neurons contain tyrosine hydroxylase, indicating that they are capable of synthesizing norepinephrine, so could

instead be adrenergic. This finding does not conform to the general understanding of peripheral autonomic nervous system organisation, in which postganglionic sympathetic cell bodies are located outside of the organs that they innervate (Nilsson, 1983; Nilsson and Holmgren, 1994). In addition to cholinergic and adrenergic neurotransmitters, other 'non-classical' autonomic transmitters have been detected within the zebrafish ICNS. Neuronal nitric oxide synthase exists in a small percentage of SAN intracardiac neurons, as well as vasoactive intestinal polypeptide in nerve terminals. The role of neurons secreting these transmitters in the zebrafish heart is not clear, but it has been suggested that intracardiac release of nitric oxide is involved in modulating cardiac effector cells (Tota et al., 2005).

A particularly intriguing finding from studies in zebrafish is the detection of what appears to be neuronal cell bodies in the ICNS, with axons projecting back to the central nervous system. These intracardiac neurons may represent afferent neurons located within the heart. Anatomical evidence for such an arrangement has been shown previously in the rat heart (Cheng et al., 1997) and electrophysiological recordings have been made from presumptive intracardiac afferent neurons in the canine heart (Ardell et al., 1991). If these labelled neurons in the zebrafish heart are in fact afferent neurons, they may provide cardio-sensory inputs to local, intracardiac control circuits, along with centrally-mediated reflex control (Stoyek et al., 2015).

Subsequent to these anatomical findings, the zebrafish isolated heart with intact extrinsic innervation has been established as a novel model for studies of autonomic control of SAN function (Stoyek et al., 2016). By combining electrocardiogram (ECG) and voltage optical mapping recordings with extrinsic nerve stimulation and pharmacological interventions, it has been demonstrated that discrete neural pathways modulate SAN function through adrenergic and cholinergic mechanisms in a similar manner to mammals [effects which are present as early as 4·days post-fertilisation (Schwerte et al., 2006)]. Using immunohistochemistry, it was further shown that SAN cells express adrenergic and cholinergic receptors, so are under direct influence of the ICNS.

Combined, these studies using zebrafish as an experimental model represent a first step towards a more comprehensive understanding of integrated autonomic control of SAN function. This model may now be utilised to identify specific relationships between subpopulations of intracardiac neurons and their targeted effector cells, which have been elusive in other experimental models, to discover basic mechanisms of intracardiac neural SAN regulation.

There is also evidence to suggest that the zebrafish may be a useful experimental model for studying the influence of NPs or stretch on SAN function. Intracardiac release of NPs in response to physiological stimuli, and their respective intracardiac receptors in zebrafish are comparable to mammals (Becker et al., 2014; Bendig et al., 2006), and preliminary experiments by our group indicate that SAN BR responses are similar to that seen in mammals. Exposure to NPs (ANP 1-28: Cat. # H-2100; BNP-32: Cat. # H5968; CNP 32-53: Cat. # H-1296; Bachem, Torrance, USA) acutely (time to peak change: 21 ± 3 s) increases BR in zebrafish isolated SAN (ANP: 24.3 ± 15.8%; BNP: 16.9 ± 10.2%; CNP: 23.1 ± 6.2%; $n = 3$ and $p < 0.05$ by two-tailed, paired Student's *t*-test, for each). Stretch-induced electrophysiological responses seen in the atria and ventricles of human are also observed in the zebrafish, and in the zebrafish SAN it has been (anecdotally) noted that stretch acutely alters SAN BR (Werdich et al., 2012).

3.2. Limitations of the zebrafish for the study of SAN function

While clear similarities in SAN function and its regulation exist between mammals and zebrafish, many fundamental mechanisms remain to be explored, and as with any experimental model, known limitations must be considered.

There are clear morphological and systemic differences between zebrafish and mammalian hearts [*e.g.*, 2 *vs.* 4 chambers, ring-*vs.* sheet-like SAN structure, low *vs.* high blood pressure (Hu et al., 2001)], but more importantly for the study of SAN function, much of what is known about basic mechanisms from mammalian studies has yet to be studied in the zebrafish. While studies of mutant zebrafish have shown that I_f is involved in SAN automaticity (Baker et al., 1997; Warren et al., 2001), the involvement of other membrane-clock mechanisms (*i.e.*, $Ca_V3.1$-mediated $I_{Ca,T}$ and $Ca_V1.3$-mediated $I_{Ca,L}$) and the Ca^{2+}-clock, as well as the relative importance of these two systems, has not been explored. It may be that pacemaking in zebrafish is primarily driven by I_f and that other membrane- and Ca^{2+}-clock mechanisms play a minimal (or non-existent) role. It is likely, however, that $Ca_V3.1$-mediated $I_{Ca,T}$ is involved, as both atrial and ventricular zebrafish cardiomyocytes display a robust current (Nemtsas et al., 2010), and possibly also $Ca_V1.3$-mediated $I_{Ca,L}$, which is expressed in zebrafish inner ear hair cells (Sidi et al., 2004) (although its presence in the zebrafish heart has not yet been established). The sparsity of SR in zebrafish myocardium (Hu et al., 2001), on the other hand, points to a potential absence of a Ca^{2+}-clock contribution to SAN automaticity. This is further supported by the limited Ca^{2+} release with excitation in zebrafish ventricular cells (Bovo et al., 2013) [along with a lack of transverse tubules (Brette et al., 2008)], although this remains controversial, as others have shown a strong dependence of contractile force on SR Ca^{2+} release (Haustein et al., 2015) and the existence of Ca^{2+} sparks with characteristics similar to mammals (Llach et al., 2011). At the same time, however, the zebrafish expresses a variety of unique Na^+-Ca^{2+} exchanger paralogs (Marshall et al., 2005), with a higher I_{NCX} than in mammals (Zhang et al., 2011), which could compensate for a lower spontaneous SR Ca^{2+} release, allowing a significant contribution of the Ca^{2+}-clock to SAN automaticity.

The presence of a host of paralogous genes in zebrafish [which is a result of the zebrafish having undergone two whole genome duplications after splitting from the phylogenetic pathway that includes humans (Howe et al., 2013)] is another potential limitation of the use of zebrafish for understanding mammalian cardiac electrophysiology, as the duplicated genes are often involved in sub-, neo-, or unknown functions. Specific to the SAN, HCN4 (the gene primarily responsible for I_f. in zebrafish and mammals) also has numerous paralogs in zebrafish (Jackson et al., 2007). While the functional impact of these paralogous genes is unclear, they may have important consequences for characteristics of I_f. One possibility is that function of the various HCN4 isoforms in zebrafish vary with temperature, which could be an important evolutionary adaptation allowing the ectothermic zebrafish to maintain SAN function over a broad range of temperatures.

The effect of temperature itself is another important consideration. It has been shown that cardiac electrophysiology in the zebrafish is extremely temperature-sensitive. In the SAN, cooling causes a reduction in the rate of DD, resulting in a 4% decrease in BR per °C drop in temperature ($Q_{10} = 1.67$), and has further direct (*i.e.*, BR-independent) effects on AP duration (Lin et al., 2014), highlighting the importance of tight temperature control for experimental studies.

3.3. Summary

Thus, the zebrafish appears to retain all critical components of intrinsic SAN regulation seen in mammals (keeping in mind known limitations), making it a potentially powerful experimental model

for studies of underlying mechanisms. However, as the SAN response to stretch in the zebrafish has not yet been systematically investigated, our goal was to examine the effects of controlled stretch on BR of the zebrafish isolated SAN, in order to evaluate its utility as a novel model for the study of intrinsic regulation by mechanical effects.

4. Methods

4.1. Ethical approval

All experimental procedures were approved by the Dalhousie University Committee for Laboratory Animals and followed the guidelines of the Canadian Council on Animal Care. Details of experimental protocols have been reported following the Minimum Information about a Cardiac Electrophysiology Experiment (MICEE) reporting standard (Quinn et al., 2011b), see online repository (https://www.micee.org/?q=node/00001379).

4.2. SAN preparation

Adult (6–12 months post-fertilisation) wild-type (AB) zebrafish were euthanised with tricaine (2 mM; E10521, Sigma-Aldrich, Oakville, Canada) in Tris-buffered (pH 7.4; BP152, Fisher Scientific, Ottawa, Canada) room temperature tank water until there was no response to fin pinch. Fish were then placed into a Sylgard-lined dish (DC 170, Dow Corning, Midland, USA) filled with Krebs-Henseleit solution (containing [in mM]: 120 NaCl, 4.7 KCl, 26 $NaHCO_3$, 1.4 NaH_2PO_4, 1.0$MgCl_2$, 1.8 $CaCl_2$, 5.0 Glucose; osmolality: 300 ± 5 mOsm/kg; pH: 7.40 ± 0.05) bubbled with carbogen (95% O_2, 5% CO_2) and maintained at 28.0 ± 0.2 °C (physiological zebrafish temperature) with a temperature-controlled (TC-344C, Warner Instruments, Hamden, USA) warmed platform (WP-16, Warner Instruments). A ventral midline incision was made through the body wall and a block of tissue encompassing the ventral aorta, ventricle, atrium, and sinus venosus was removed and placed in a separate dish. In the two-chambered zebrafish heart, the SAN is arranged in an oval ring that surrounds the orifice between the sinus venosus and the atrium. To expose the SAN, the ventricle was removed and the atrium cut open and pinned flat. A custom suction microelectrode (1.00/0.58 mm outer/inner diameter; 1B100 and MPH6R10, World Precision Instruments, Sarasota, USA) connected to an ECG amplifier (Animal Bio Amp, ADInstruments, Colorado Springs, USA) was positioned with a three-axis rack and pinion stage (62041, Edmond Optics, Barrington, USA) at the edge of the atrium and suction applied with a 1 ml syringe to measure the local ECG. Bath temperature was measured using a thermocouple (T-type pod, ADInstruments). Temperature and ECG signals were recorded at 2000 Hz using a data acquisition device (PowerLab, ADInstruments) controlled by LabChart (ADInstruments; Fig. 3).

4.3. SAN stretch

Two custom-made micro-sized hooks (~100 μm in diameter; Fig. 1B) fashioned from single-barrel borosilicate glass capillaries (2.00/1.12 mm outer/inner diameter; 1B200F, World Precision Instruments) were coupled with microelectrode holders (MPH110, World Precision Instruments) to independent three-axis hydraulic micromanipulators (for fine positioning; MHW-103, Narishige International, East Meadow, USA) mounted on piezoelectric linear translators (for application of sub-nanometer resolution stretch; P-621.1CD, Physik Instrumente, Auburn, USA) fixed to stages on a rack and pinion track (for coarse positioning; 56798, Edmond Optics). The hooks were inserted opposing each other into the SAN ring in the long- or short-axis direction ($n = 13$ for each; Fig. 2A), such that the tissue rested within the loops of the hooks (*i.e.*, without tissue puncture/damage), using the micromanipulators under an upright microscope (BX63, Olympus, Richmond Hill, Canada) with a 5 × objective (Fig. 1A). Piezoelectric position was controlled by a servo controller (E-665.CR, Physik Instrumente) driven by a data acquisition device (USB-6361, National Instruments, Austin, USA) with custom routines developed in LabView (National Instruments) to apply precise magnitudes of stretch (10, 25, or 50%; Fig. 2B–C) to the SAN.

4.4. Experimental protocol

Preparations with hooks in either the long- or short-axis direction were left to equilibrate for 30 min to ensure a stable baseline BR. The hooks were separated using the micromanipulators to the point at which each hook made contact with, and just began to stretch the SAN. The pre-stretch distance between the hooks was measured and this distance was increased by 10% at a rate of 1 mm/s by moving both piezoelectric translators. Stretch was maintained for 30 s followed by return to the pre-stretch distance at the same rate as stretch. After 120 s of rest the stretch protocol was repeated three times (Fig. 3), followed by a repetition of the entire stretch procedure with 25 and 50% increase in inter-hook distance (for a total of 12 stretches). The two piezoelectric translator positions were recorded at 2000 Hz with the data acquisition device.

4.5. Data analysis

Data analysis was performed using custom routines in Matlab (MathWorks, Natick, USA). BR was calculated from the peaks of the ECG signal and stretch percentage from the two piezoelectric translator positions (Fig. 3). Baseline BR was measured as the average BR during the rest period prior to each stretch. With stretch, average BR was measured over the entire 30 s stretch period and peak BR was averaged over eleven beats centred on the maximum BR. Time to peak response was measured as the time from stretch initiation to the maximum BR. Heart rate variability (HRV) was assessed during the baseline and stretch periods by calculating the standard deviation of BR and the root mean square of the successive differences in BR.

Statistical analysis was performed in SPSS (IBM, Armonk, USA). Values are presented as mean ± standard error of the mean, with a p-value < 0.05 indicating significance. Three factors related to the stretch response were considered: (i) stretch magnitude (10 *vs*. 25 *vs*. 50%), (ii) temporal response (average *vs*. peak), and (iii) direction of stretch (long- *vs*. short-axis). Two-way repeated-measures ANOVA was used to assess: (i) the effect of stretch magnitude, by comparing baseline, average, and peak BR; (ii) the temporal response, by comparing average and peak percentage change in BR; and (iii) HRV at baseline and with stretch, at each stretch magnitude in the long- and short-axis direction. Two-way mixed ANOVA was used to assess the influence of stretch direction by comparing peak percentage change in BR for long- and short-axis stretch at each stretch magnitude. One-way repeated measures ANOVA was used to compare time to peak BR at each stretch magnitude in the long- and short-axis direction. Greenhouse-Geisser correction for non-sphericity was applied when appropriate, significant main effects were analysed by Bonferroni *post hoc* tests, and when the interaction effect was significant, simple effects were analysed by Student's *t*-test. SAN ring diameter and average time to peak BR for long- and short-axis stretch were compared by two-tailed, unpaired Student's *t*-test and initial and final temperature were compared by two-tailed, paired Student's *t*-test. The relationship between the peak change in BR and its baseline value was assessed by linear correlation.

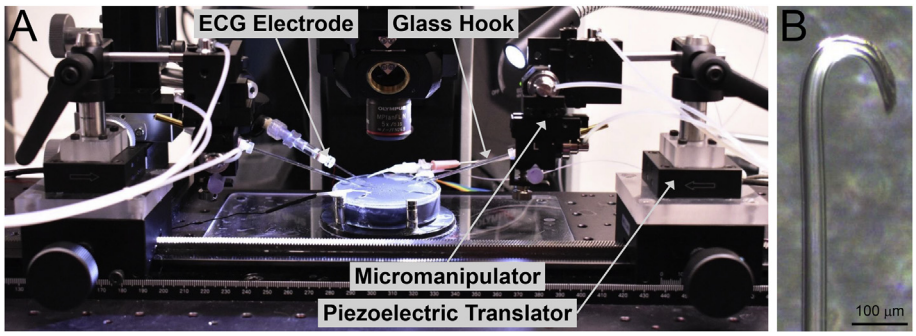

Fig. 1. (A) Experimental setup showing three-axis hydraulic micromanipulators mounted on piezoelectric linear translators for positioning and controlled manipulation of micro-sized hooks inserted into the zebrafish isolated sinoatrial node (SAN) ring, with electrocardiogram (ECG) measured by a suction microelectrode. This was performed in a heated and bubbled bath under an upright microscope with a 5 × objective. (B) Custom-made micro-sized hooks fashioned from single-barrel borosilicate glass capillaries.

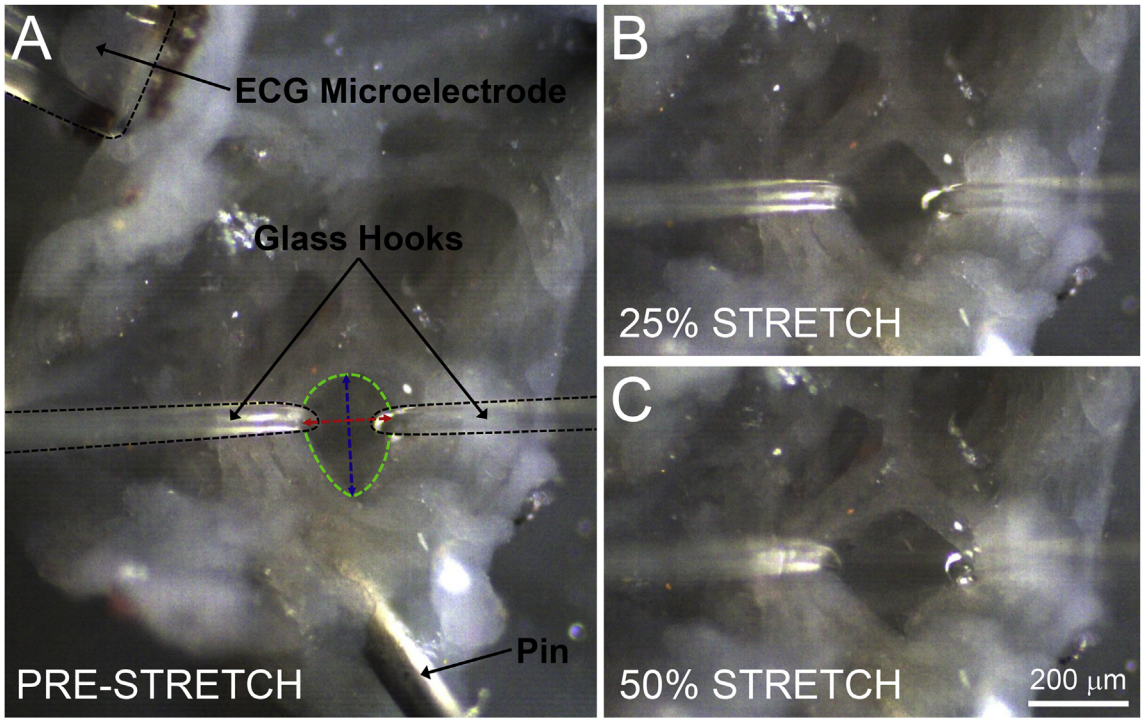

Fig. 2. (A) Zebrafish isolated atrium pinned flat to expose the oval sinoatrial node (SAN) ring (outlined by green dashed line), in which glass hooks have been inserted opposing each other in the short-axis direction (indicated by red dashed line, with long-axis indicated by blue dashed line) and separated to the pre-stretch position, with ECG measured by a suction microelectrode. (B) 25% and (C) 50% short-axis SAN stretch.

5. Results

Before commencing the stretch protocol, all isolated SAN preparations displayed regular spontaneous beating (140 ± 5 beats/min; $n = 26$). Before long-axis stretch, the diameter of the SAN ring was 220 ± 11 μm. With stretch in this direction, BR immediately began to increase (Fig. 3), reaching a peak on average after 16 ± 1 s, which did not vary with stretch magnitude (10%: 14.8 ± 1.5 s; 25%: 16.5 ± 1.7 s; 50%: 15.6 ± 2.0 s; $n = 13$, $p = 0.68$). For short axis stretch, the initial diameter of the SAN ring was not different than for long-axis stretch (220 ± 13 μm, $p = 0.989$) and, the time to peak BR was also not dependent on stretch magnitude (10%: 17.8 ± 1.5 s; 25%: 19.8 ± 1.6 s; 50%: 18.3 ± 2.0 s; $n = 13$, $p = 0.62$), although the average time to peak BR (18.6 ± 1.0 s) was longer than for long-axis stretch ($p = 0.03$). Upon release, BR began to immediately decrease, returning to baseline over a similar time course as the increase with stretch (Fig. 3).

The temporal effect-stretch magnitude interaction was significant for both long- and short-axis stretch ($p = 0.042$ and 0.021, respectively). For long-axis stretch, peak BR after stretch was greater than baseline for all stretch magnitudes, while average BR was only greater than baseline for 50% stretch (Fig. 4). For short-axis stretch, both average and peak BR were greater than baseline for all stretch magnitudes, and both were greater for 50% stretch than for 10 or 25%. Across the stretch protocol there was no change in baseline BR (Fig. 4) or temperature (initial: 28.4 ± 0.2 °C, final: 27.9 ± 0.2 °C, $p = 0.18$), and the peak change in BR was not related to baseline BR (all R^2-values < 0.1).

Fig. 5 shows the absolute peak and average change in BR for long- and short-axis stretch, demonstrating the temporal- (average *vs.* peak) and stretch direction- (long- *vs.* short-axis) dependence of stretch effects. For comparison, changes in BR were normalised to the pre-stretch value by calculating the percentage change in BR. The temporal effect-stretch magnitude interaction was significant

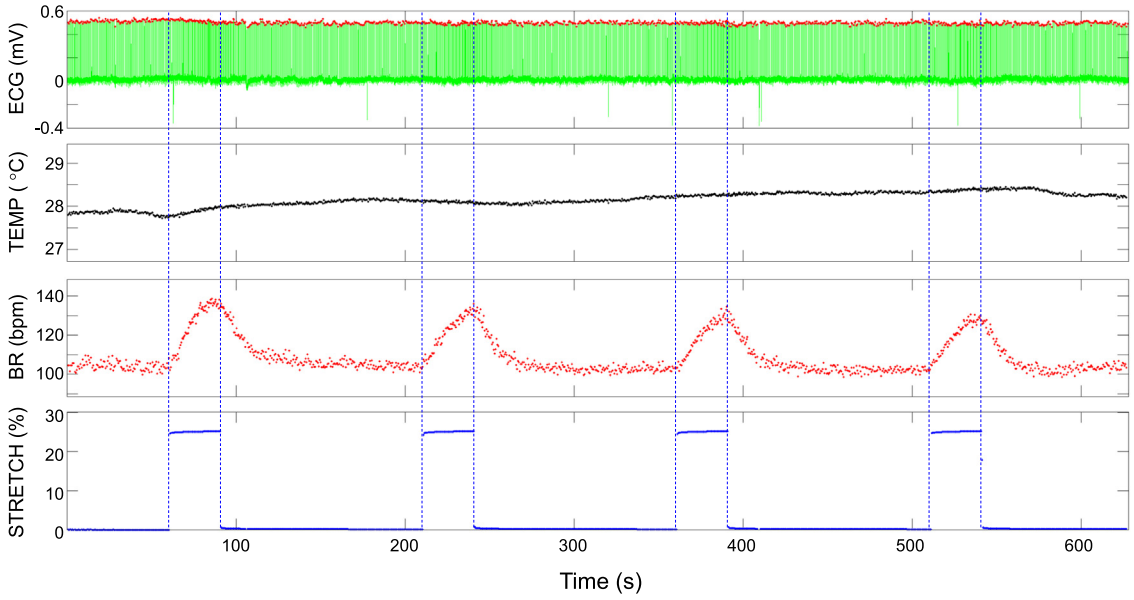

Fig. 3. Representative electrocardiogram (ECG), temperature (TEMP), beating rate (BR), and stretch magnitude (STRETCH) signals for four repetitions of 25% short-axis stretch.

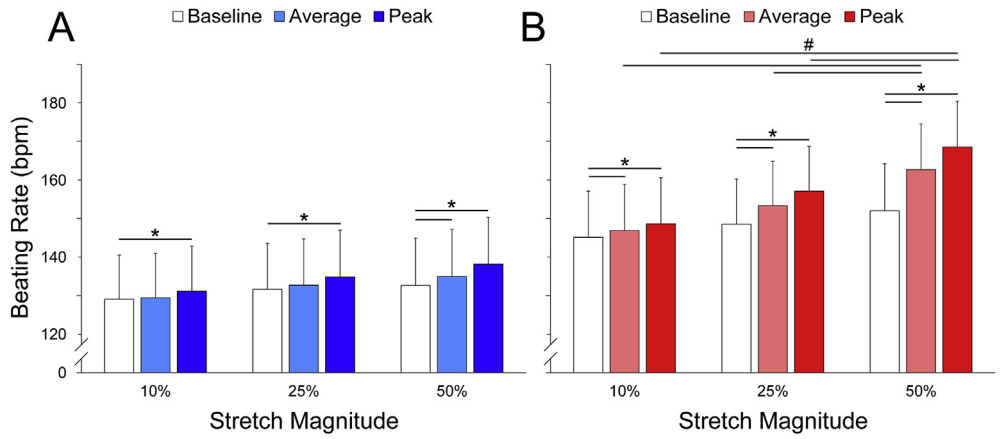

Fig. 4. Baseline, average, and peak beating rate for 10, 25, and 50% stretch in the (A) long-axis and (B) short-axis direction. *p < 0.05 for average *vs.* baseline and #p < 0.05 for 50% *vs.* 10 or 25%.

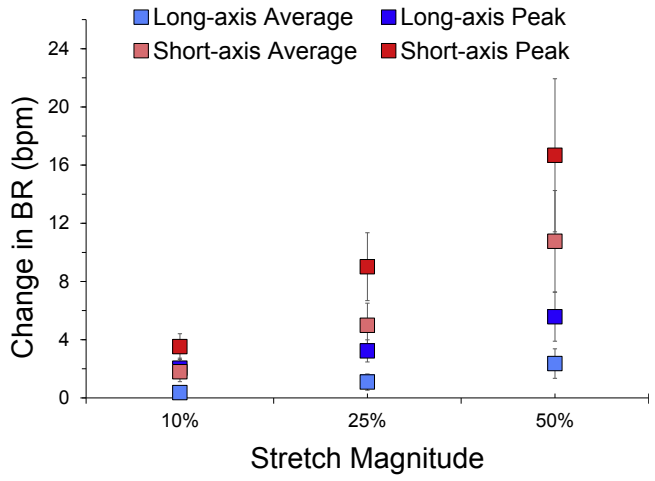

Fig. 5. Absolute average and peak change in beating rate (BR) for 10, 25, and 50% stretch in the long-axis and short-axis direction.

for short-axis stretch only ($p = 0.039$), with a greater peak than average percentage change in BR for all stretch magnitudes (Fig. 6), reflecting the continuous increase in rate during the stretch period. Further, the direction-stretch magnitude interaction was significant ($p = 0.013$), with a greater peak percentage change in BR for 25% stretch in the short compared to long-axis direction (Fig. 7).

For HRV measured by the standard deviation of BR, the stretch-stretch magnitude interaction effect was significant for both long- and short-axis stretch ($p = 0.003$ and 0.016, respectively). HRV decreased for 10% stretch in both the long- and short-axis direction and increased for 50% stretch in the long-axis direction (Fig. 8). No differences were seen in the root mean square of the successive differences of BR.

6. Discussion

We performed a systematic investigation of the response of the zebrafish isolated SAN to varying degrees of controlled stretch. Overall, it was found that stretch causes an immediate and continuous increase in BR, which reaches a maximum part way

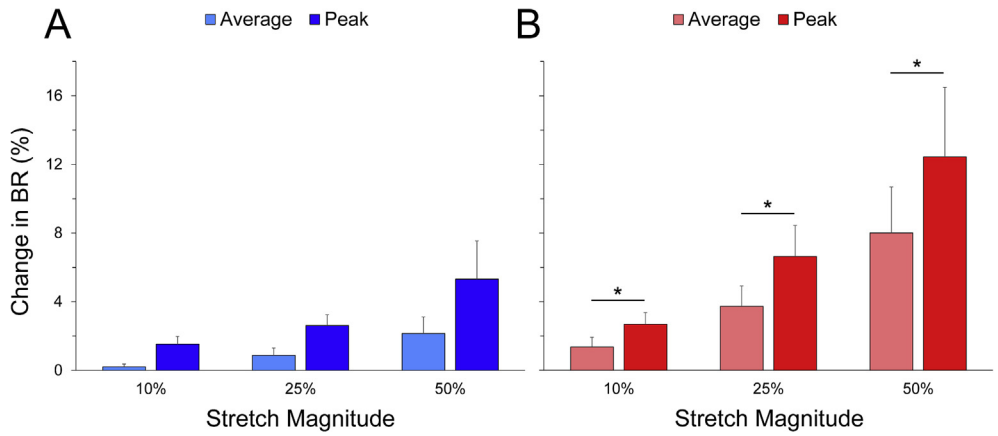

Fig. 6. Average and peak percentage change in beating rate (BR) for 10, 25, and 50% stretch in the (A) long-axis and (B) short-axis direction. *p < 0.005 for peak *vs.* average.

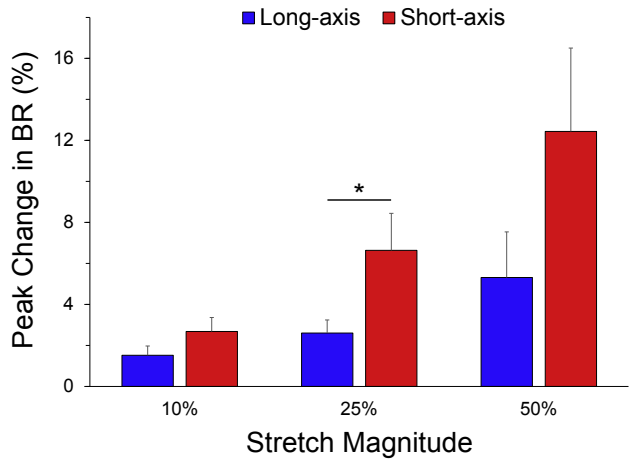

Fig. 7. Peak percentage change in beating rate (BR) for 10, 25, and 50% stretch in the long-axis and short-axis direction. *p < 0.05 for short-axis *vs.* long-axis.

through a period of sustained stretch, and the extent of which is dependent on the magnitude and direction of stretch. This chronotropic response is comparable to what occurs in isolated SAN from most mammals (although not from mice), suggesting that the zebrafish may represent a novel experimental model for the study of mechanisms involved in the intrinsic regulation of SAN function by mechanical effects.

6.1. Determinants of the response to stretch

The increase in BR with stretch in our experiments was magnitude-, direction-, and time-dependent. The importance of stretch magnitude is well established from previous work (Quinn and Kohl, 2012), yet it remains unknown whether: (i) the key mechanical parameter is strain (stretch) (Kamiyama et al., 1984; Sanders et al., 1979), stress (tension) (Arai et al., 1996; Brooks et al., 1966; Chiba, 1977; Cooper and Kohl, 2005), or a combination of both (Lange et al., 1966); (ii) the response is dependent (Brooks et al., 1966; Lange et al., 1966) or independent (Chiba, 1977) of stretch rate; or (iii) there is an effect of the spatial nature of stretch (*i.e.*, linear, biaxial, or concentric) (Deck, 1964). The dependence on stretch direction in our experiments may reflect an influence of anisotropic tissue properties, which could affect the spatial distribution of stress and/or strain across the SAN tissue. To address this, it is essential that future experiments include the measurement of applied force during stretch, which will also provide insight into the dependence of the increase in BR on stress *vs.* strain. It may also help reduce the relatively large inter-subject variability of the stretch-induced change in BR seen in our experiments, as pre-stretch hook separation may be more consistently determined by pre-stretch force.

Our experiments demonstrated that while BR immediately began to increase with stretch, there was a delay to the peak response, and that the return of BR to baseline after release occurred over a similar timescale. This finding may also be explained by mechanical properties of the SAN, as a consequence of visco-elastic dampening of the translation of applied stress into tissue stretch, as well as its decline after release. Alternatively, it may point to the involvement of a (more slowly activating) second messenger system in the stretch-induced response to BR, which requires time for removal after a return to normal tissue length. An important consequence of this temporal aspect of the stretch response is that the change in BR averaged over the entire stretch period will be lower than the peak response, which complicates comparison of previous studies that involved different stretch durations and measurements of BR.

The temporal nature of the stretch response also highlights the importance of stretch timing. In ventricular myocytes, it has been shown that stretch effects on the AP are phase-dependent (Calkins et al., 1991; Franz et al., 1992; Hansen et al., 1990; Nishimura et al., 2008). This means that the timing of stretch application must be controlled to mimic desired physiological and pathophysiological states. In the case of the SAN, under normal conditions stretch will be greatest at the end of atrial filling, which is when SAN cells are moving towards AP initiation. In this way, 'mechanical priming' of SAN cells could adjust function on a beat-by-beat basis to diastolic load, contributing to the matching of cardiac output (BR × stroke volume) to venous return. In pathophysiological conditions that involve dyssynchronous contraction, on the other hand, systolic/early diastolic stretch could occur, which will affect cell repolarisation, potentially slowing BR and destabilising function. Past studies (including the present investigation), however, have utilised sustained (and often excessive) stretch. Studies investigating the effects of stretch timed with distinct phases of the cardiac cycle are needed to understand the physiological importance of the chronotropic response to stretch.

Phase-dependent effects may also explain the observed species-dependence of the response to sustained stretch [*i.e.*, increased BR in most mammals, but a decrease in mice (Cooper and Kohl, 2005)]. Assuming activation of SAC_{NS} is primarily responsible for changes in BR in both cases, in SAN from animals with APs characterised by a

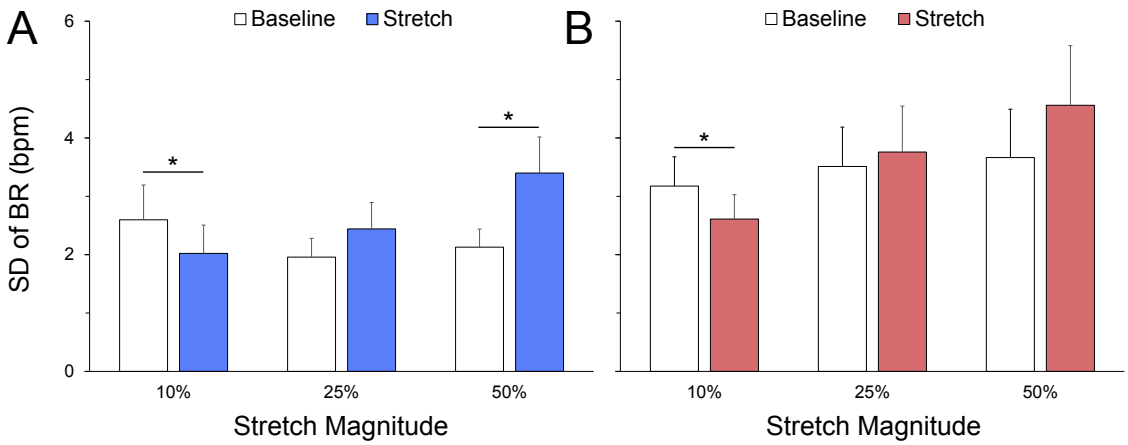

Fig. 8. Standard deviation (SD) of beating rate (BR) at baseline and during 10, 25, and 50% stretch in the (A) long-axis and (B) short-axis direction. *$p < 0.05$ for stretch *vs.* baseline.

relatively slow upstroke and prominent plateau-like early repolarisation phase (with V_m moving away from the reversal potential of SAC_{NS} [~-10 mV] during a larger proportion of each cycle), sustained stretch will more often accelerate changes in V_m (by pulling V_m in the direction of the reversal potential), thus increasing BR (Fig. 9A). In SAN from mice (with faster upstrokes, often carried by a mix of Na^+ and Ca^{2+} currents (Lei et al., 2007), and a swift initial repolarisation), on the other hand, sustained stretch will do the opposite (Fig. 9B). This theory fits with our results found in the zebrafish, as zebrafish AP morphologies are closer to large mammals than mice (Nemtsas et al., 2010), so would be expected to have an increase in BR with sustained stretch (Fig. 9C). One should use caution, however, when generalising the shape of SAN APs from different species, as heterogeneity in SAN cell electrophysiology results in spatially-varying AP morphologies (Boyett et al., 2000; Monfredi et al., 2010), resulting in an overlap between mice and other mammals. While SAN cells from larger mammals generally display longer APs, central SAN cells from mice have very little detectable Na^+ current and slower upstrokes, while peripheral SAN cells in larger mammals often display rapid upstrokes. It is difficult to predict how SAN cell heterogeneity will contribute to the stretch response in the intact SAN; a spatial assessment of APs in the zebrafish SAN may help determine its importance. That said, from the chronotropic response measured in the present work, it appears that the zebrafish represents an appropriate experimental model for the investigation of the effects and relevance of timed SAN stretch, and to test the species-dependence hypothesis.

6.2. Mechanisms of the response to stretch

As SAC_{NS} activity in myocytes can account for the electrophysiological changes that occur with stretch of the SAN, and their pharmacological block causes a reversible reduction of the stretch-induced change in BR (Cooper and Kohl, 2005), they have been implicated as the primary mediator of stretch effects. Yet, while a long list of candidates exist, their molecular identity remains unknown (Peyronnet et al., 2016). As zebrafish display stretch responses, and powerful tools exist for their genetic modification, they may represent a useful experimental model for determining the identity of SAC_{NS}. Of course, mechanisms other than SAC_{NS} activation in myocytes may be involved in stretch responses. For instance, SAC_{NS} in fibroblasts, if coupled to myocytes, may contribute. Here again the zebrafish may be a powerful experimental tool, as by cell-specific expression of genetically-encoded voltage-sensitive fluorescent proteins one can probe the role of different cell types in electrophysiological responses (Quinn et al., 2016). Fluorescent-based optical mapping techniques may also prove useful for investigating the effects of stretch on AP morphology, Ca^{2+} handling, or the pattern of SAN excitation.

Stretch effects may also be conferred by mechano-sensitivity of other components of the V_m/Ca^{2+} pacemaking system, such as HCN channels or internal Ca^{2+} handling, or other intrinsic regulatory

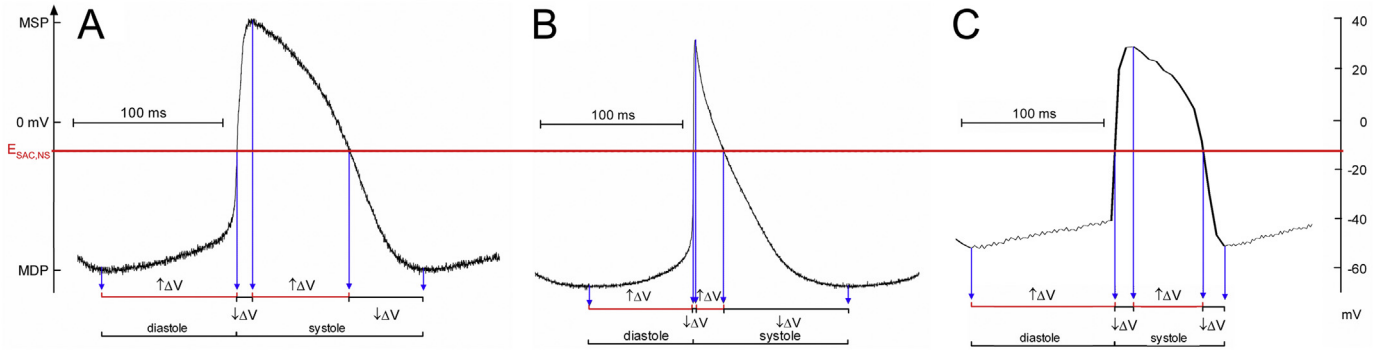

Fig. 9. Theoretical effects of cation non-selective stretch-activated channels (SAC,NS) on the sinoatrial node action potential of (A) rabbit, (B) mouse, and (C) zebrafish. Experimental membrane potential recordings from each species show the relation of electrophysiological parameters (maximum diastolic and systolic membrane potential, MDP and MSP, respectively) and SAC,NS reversal potential ($E_{SAC,NS}$). The time periods during which SAC,NS activity would either accelerate (↑ΔV) or slow (↓ΔV) changes in membrane potential are indicated. In rabbit and zebrafish, SAC,NS would accelerate changes in membrane potential during ~70 and 80% of the action potential, respectively, while in mouse this would occur over only ~45% of the action potential. Adapted (with addition of zebrafish recording) from (Cooper and Ravens, 2011), with permission.

pathways, such as interactions with autonomic BR modulation (Barrett et al., 1998; Bolter, 1994, 1996; Bolter and Wilson, 1999; Wilson and Bolter, 2001) or local stretch-induced release of NPs (de Bold et al., 1996). In the zebrafish these possibilities may be investigated using genetic or pharmacological techniques, and may further benefit from computational modelling for quantitative assessment of their plausibility, experimentally-testable prediction and hypothesis generation, and ultimately integration of findings and their projection across relevant species and spatial/temporal scales (Muszkiewicz et al., 2016; Quinn and Kohl, 2013).

6.3. Relevance for normal and pathophysiological function

Intrinsic regulation of SAN function by mechanical factors is an area which deserves greater attention, as *in vivo* the SAN is continuously subjected to cyclic variations in hemodynamic load, while isolated cells – the principal experimental model for insight into the molecular mechanisms of pacemaker function – have mostly been studied in unloaded conditions. For instance, it appears that physiological loading may be essential to normal SAN automaticity, as slack tissue often shows no or irregular rhythm, while moderate stretch can restore normal activity (Brooks et al., 1966). This apparent requirement for a minimum mechanical stimulus is also apparent during ontogenetic initiation of the first heartbeat, as fluid pressure build-up in the quiescent cardiac tube appears to be required for the initiation of its spontaneous activity (Chiou et al., 2016; Rajala et al., 1977). Moreover, the adjustment of BR to diastolic filling is essential for the matching of cardiac output (BR × stroke volume) to changes in venous return.

The mechanical regulation of BR works, however, only within a particular range of stretch. After an initial acceleration in BR, excessive stretch can unbalance pacemaker function, inducing arrhythmias (Brooks et al., 1966; Hoffman and Cranefield, 1960). This pathophysiological response may be important in diseases associated with atrial volume overload (Morton et al., 2003; Sanders et al., 2003; Sparks et al., 1999), atrial fibrillation (Elvan et al., 1996; Kumagai et al., 1991), advanced age (Mohler and Anderson, 2008; Rubenstein et al., 1972), or other cardiac pathologies (Akoum et al., 2012; Bockstall and Link, 2012; Kottkamp, 2012; Nakao et al., 2012) that are accompanied by SAN dysfunction, especially in cases where increased fibrosis will alter SAN mechanical properties and the distribution of stretch (interestingly, with similar mechanical load, changes in BR are greater in SAN preparations from younger animals (Deck, 1964), in which generally less fibrosis is present). This will be further exacerbated if fibroblast mechano-sensitivity plays a role in SAN stretch-responses.

Another potentially important consequence of changes in SAN mechanical loading is impacts on HRV. HRV is generally thought to be an index of autonomic function and decreased HRV is an independent predictor of cardiac morbidity and mortality in patients suffering from various forms of heart disease (Task Force of the European Society of Cardiology and the North American Society of Pacing and Electrophysiology, 1996). It has been shown previously that in patients with atrial overload secondary to pulmonary arterial hypertension (McGowan et al., 2009), or in anesthetised pigs with targeted right-atrial distension (Horner et al., 1996), HRV is reduced. In agreement with these previous findings, we found that 10% stretch was associated with a decrease in HRV. With greater stretch (50% in the short-axis direction), however, HRV was increased. The reason for this discrepancy may relate to differences in stretch characteristics (for instance stretch duration, which was an order of magnitude shorter in our experiments than in the pig), chronic *vs.* acute effects, or preparation- (isolated *vs.* intact heart) or species-related differences. Intriguingly, as we used isolated (and thus decentralised) hearts in our experiments, changes in HRV may have represented changes in intrinsic (rather than centrally-mediated) ICNS-based regulation of SAN function.

7. Conclusion

The zebrafish isolated SAN responds to stretch in a similar manner to human (and most other mammals), with an immediate magnitude-dependent increase in BR. This is an important mechanism for intrinsic regulation of SAN function, which allows the heart to adapt to changes in hemodynamic load on a beat-by-beat basis. Yet, the mechanism of this positive chronotropic response is unknown, due in part to the lack of an appropriate genetically modifiable species for targeted investigations. The zebrafish, with its functional and genetic similarities to human, and the relative ease of its genetic modification, represents an alternative experimental model for the study of intrinsic regulation of SAN function.

Acknowledgements

This work was supported by the Natural Sciences and Engineering Research Council of Canada (RGPIN-2015-04759 and RGPIN-2016-04879 to TAQ), the Canada Foundation for Innovation (project number 32962), and the Dalhousie Medical Research Foundation. RAR's research program is supported by the Canadian Institutes of Health Research (MOP 93718) and the Heart and Stroke Foundation of Canada (HSFC). TAQ is a National New Investigator of the HSFC.

References

Abraham, R.L., Yang, T., Blair, M., Roden, D.M., Darbar, D., 2010. Augmented potassium current is a shared phenotype for two genetic defects associated with familial atrial fibrillation. J. Mol. Cell Cardiol. 48, 181–190.

Akoum, N., McGann, C., Vergara, G., Badger, T., Ranjan, R., Mahnkopf, C., Kholmovski, E., Macleod, R., Marrouche, N., 2012. Atrial fibrosis quantified using late gadolinium enhancement MRI is associated with sinus node dysfunction requiring pacemaker implant. J. Cardiovasc Electrophysiol. 23, 44–50.

Anand-Srivastava, M.B., 2005. Natriuretic peptide receptor-C signaling and regulation. Peptides 26, 1044–1059.

Arai, A., Kodama, I., Toyama, J., 1996. Roles of Cl^- channels and Ca^{2+} mobilization in stretch-induced increase of SA node pacemaker activity. Am. J. Physiol. 270, H1726–H1735.

Ardell, J.L., Armour, J.A., 2016. Neurocardiology: structure-based function. Compr. Physiol. 6, 1635–1653.

Ardell, J.L., Butler, C.K., Smith, F.M., Hopkins, D.A., Armour, J.A., 1991. Activity of in vivo atrial and ventricular neurons in chronically decentralized canine hearts. Am. J. Physiol. 260, H713–H721.

Ardell, J.L., Cardinal, R., Beaumont, E., Vermeulen, M., Smith, F.M., Andrew Armour, J., 2014. Chronic spinal cord stimulation modifies intrinsic cardiac synaptic efficacy in the suppression of atrial fibrillation. Auton. Neurosci. 186, 38–44.

Armour, J.A., 2008. Potential clinical relevance of the 'little brain' on the mammalian heart. Exp. Physiol. 93, 165–176.

Armour, J.A., Ardell, J.L., 2004. Basic and Clinical Neurocardiology. Oxford University Press.

Armour, J.A., Murphy, D.A., Yuan, B.X., Macdonald, S., Hopkins, D.A., 1997. Gross and microscopic anatomy of the human intrinsic cardiac nervous system. Anat. Rec. 247, 289–298.

Arrenberg, A.B., Stainier, D.Y., Baier, H., Huisken, J., 2010. Optogenetic control of cardiac function. Science 330, 971–974.

Azer, J., Hua, R., Vella, K., Rose, R.A., 2012. Natriuretic peptides regulate heart rate and sinoatrial node function by activating multiple natriuretic peptide receptors. J. Mol. Cell Cardiol. 53, 715–724.

Azer, J., Hua, R., Krishnaswamy, P.S., Rose, R.A., 2014. Effects of natriuretic peptides on electrical conduction in the sinoatrial node and atrial myocardium of the heart. J. Physiol. 592, 1025–1045.

Bainbridge, F.A., 1915. The influence of venous filling upon the rate of the heart. J. Physiol. 50, 65–84.

Baker, K., Warren, K.S., Yellen, G., Fishman, M.C., 1997. Defective "pacemaker" current (Ih) in a zebrafish mutant with a slow heart rate. Proc. Natl. Acad. Sci. U. S. A. 94, 4554–4559.

Barrett, C.J., Bolter, C.P., Wilson, S.J., 1998. The intrinsic rate response of the isolated right atrium of the rat, Rattus norvegicus. Comp. Biochem. Physiol. A Mol. Integr. Physiol. 120, 391–397.

Beaulieu, P., Lambert, C., 1998. Peptidic regulation of heart rate and interactions with the autonomic nervous system. Cardiovasc Res. 37, 578–585.
Becker, J.R., Chatterjee, S., Robinson, T.Y., Bennett, J.S., Panakova, D., Galindo, C.L., Zhong, L., Shin, J.T., Coy, S.M., Kelly, A.E., Roden, D.M., Lim, C.C., MacRae, C.A., 2014. Differential activation of natriuretic peptide receptors modulates cardiomyocyte proliferation during development. Development 141, 335–345.
Belmonte, S., Morad, M., 2008. 'Pressure-flow'-triggered intracellular Ca^{2+} transients in rat cardiac myocytes: possible mechanisms and role of mitochondria. J. Physiol. 586, 1379–1397.
Bendig, G., Grimmler, M., Huttner, I.G., Wessels, G., Dahme, T., Just, S., Trano, N., Katus, H.A., Fishman, M.C., Rottbauer, W., 2006. Integrin-linked kinase, a novel component of the cardiac mechanical stretch sensor, controls contractility in the zebrafish heart. Genes Dev. 20, 2361–2372.
Blaschke, R.J., Hahurij, N.D., Kuijper, S., Just, S., Wisse, L.J., Deissler, K., Maxelon, T., Anastassiadis, K., Spitzer, J., Hardt, S.E., Scholer, H., Feitsma, H., Rottbauer, W., Blum, M., Meijlink, F., Rappold, G., Gittenberger-de Groot, A.C., 2007. Targeted mutation reveals essential functions of the homeodomain transcription factor Shox2 in sinoatrial and pacemaking development. Circulation 115, 1830–1838.
Blinks, J.R., 1956. Positive chronotropic effect of increasing right atrial pressure in the isolated mammalian heart. Am. J. Physiol. 186, 299–303.
Bockstall, K.E., Link, M.S., 2012. A primer on arrhythmias in patients with hypertrophic cardiomyopathy. Curr. Cardiol. Rep. 14, 552–562.
Bolter, C.P., 1994. Intrinsic cardiac rate regulation in the anaesthetized rabbit. Acta Physiol. Scand. 151, 421–428.
Bolter, C.P., 1996. Effect of changes in transmural pressure on contraction frequency of the isolated right atrium of the rabbit. Acta Physiol. Scand. 156, 45–50.
Bolter, C.P., Wilson, S.J., 1999. Influence of right atrial pressure on the cardiac pacemaker response to vagal stimulation. Am. J. Physiol. 276, R1112–R1117.
Bovo, E., Dvornikov, A.V., Mazurek, S.R., de Tombe, P.P., Zima, A.V., 2013. Mechanisms of Ca(2)+ handling in zebrafish ventricular myocytes. Pflugers Arch. 465, 1775–1784.
Boyett, M.R., Honjo, H., Kodama, I., 2000. The sinoatrial node, a heterogeneous pacemaker structure. Cardiovasc Res. 47, 658–687.
Brette, F., Luxan, G., Cros, C., Dixey, H., Wilson, C., Shiels, H.A., 2008. Characterization of isolated ventricular myocytes from adult zebrafish (Danio rerio). Biochem. Biophys. Res. Commun. 374, 143–146.
Brooks, C.M., Lange, G., 1977. Interaction of myogenic and neurogenic mechanisms that control heart rate. Proc. Natl. Acad. Sci. U. S. A. 74, 1761–1762.
Brooks, C.M., Lu, H.H., Lange, G., Mangi, R., Shaw, R.B., Geoly, K., 1966. Effects of localized stretch of the sinoatrial node region of the dog heart. Am. J. Physiol. 211, 1197–1202.
Calabrese, B., Tabarean, I.V., Juranka, P., Morris, C.E., 2002. Mechanosensitivity of N-type calcium channel currents. Biophys. J. 83, 2560–2574.
Calkins, H., Levine, J.H., Kass, D.A., 1991. Electrophysiological effect of varied rate and extent of acute in vivo left ventricular load increase. Cardiovasc Res. 25, 637–644.
Calloe, K., Elmedyb, P., Olesen, S.P., Jorgensen, N.K., Grunnet, M., 2005. Hypoosmotic cell swelling as a novel mechanism for modulation of cloned HCN2 channels. Biophys. J. 89, 2159–2169.
Camelliti, P., Green, C.R., LeGrice, I., Kohl, P., 2004. Fibroblast network in rabbit sinoatrial node: structural and functional identification of homogeneous and heterogeneous cell coupling. Circ. Res. 94, 828–835.
Cheng, Z., Powley, T.L., Schwaber, J.S., Doyle 3rd, F.J., 1997. Vagal afferent innervation of the atria of the rat heart reconstructed with confocal microscopy. J. Comp. Neurol. 381, 1–17.
Chiba, S., 1977. Pharmacologic analysis of stretch-induced sinus acceleration of the isolated dog atrium. Jpn. Heart J. 18, 398–405.
Chiou, K.K., Rocks, J.W., Chen, C.Y., Cho, S., Merkus, K.E., Rajaratnam, A., Robison, P., Tewari, M., Vogel, K., Majkut, S.F., Prosser, B.L., Discher, D.E., Liu, A.J., 2016. Mechanical signaling coordinates the embryonic heartbeat. Proc. Natl. Acad. Sci. U. S. A. 113, 8939–8944.
Cooper, P.J., Kohl, P., 2005. Species- and preparation-dependence of stretch effects on sino-atrial node pacemaking. Ann. N. Y. Acad. Sci. 1047, 324–335.
Cooper, P.J., Ravens, U., 2011. Mechanical modulation of pacemaker electrophysiology. In: Kohl, P., Sachs, F., Franz, M.R. (Eds.), Cardiac Mechano-electric Coupling and Arrhythmias. Oxford University Press, Oxford, pp. 95–102.
Cooper, P.J., Lei, M., Cheng, L.X., Kohl, P., 2000. Selected contribution: axial stretch increases spontaneous pacemaker activity in rabbit isolated sinoatrial node cells. J. Appl. Physiol. 89, 2099–2104.
Craelius, W., Chen, V., el-Sherif, N., 1988. Stretch activated ion channels in ventricular myocytes. Biosci. Rep. 8, 407–414.
de Bold, A.J., Bruneau, B.G., Kuroski de Bold, M.L., 1996. Mechanical and neuroendocrine regulation of the endocrine heart. Cardiovasc Res. 31, 7–18.
Deck, K.A., 1964. Dehnungseffekte am spontanschlagenden, isolierten Sinusknoten. Pflugers Arch. Gesamte Physiol. Menschen Tiere 280, 120–130.
DiFrancesco, D., 1993. Pacemaker mechanisms in cardiac tissue. Annu. Rev. Physiol. 55, 455–472.
DiFrancesco, D., 2006. Funny channels in the control of cardiac rhythm and mode of action of selective blockers. Pharmacol. Res. 53, 399–406.
DiFrancesco, D., 2010. The role of the funny current in pacemaker activity. Circ. Res. 106, 434–446.
DiFrancesco, D., Noble, D., 2012. The funny current has a major pacemaking role in the sinus node. Heart Rhythm 9, 299–301.
Donald, D.E., Shepherd, J.T., 1978. Reflexes from the heart and lungs: physiological curiosities or important regulatory mechanisms. Cardiovasc Res. 12, 446–469.
Egom, E.E., Vella, K., Hua, R., Jansen, H.J., Moghtadaei, M., Polina, I., Bogachev, O., Hurnik, R., Mackasey, M., Rafferty, S., Ray, G., Rose, R.A., 2015. Impaired sinoatrial node function and increased susceptibility to atrial fibrillation in mice lacking natriuretic peptide receptor C. J. Physiol. 593, 1127–1146.
Elvan, A., Wylie, K., Zipes, D.P., 1996. Pacing-induced chronic atrial fibrillation impairs sinus node function in dogs. Electrophysiological remodeling. Circulation 94, 2953–2960.
Fischmeister, R., Castro, L.R., Abi-Gerges, A., Rochais, F., Jurevicius, J., Leroy, J., Vandecasteele, G., 2006. Compartmentation of cyclic nucleotide signaling in the heart: the role of cyclic nucleotide phosphodiesterases. Circ. Res. 99, 816–828.
Franz, M.R., Cima, R., Wang, D., Profitt, D., Kurz, R., 1992. Electrophysiological effects of myocardial stretch and mechanical determinants of stretch-activated arrhythmias. Circulation 86, 968–978.
Gagliardi, M., Randall, W.C., Bieger, D., Wurster, R.D., Hopkins, D.A., Armour, J.A., 1988. Activity of in vivo canine cardiac plexus neurons. Am. J. Physiol. 255, H789–H800.
Gamble, J., Taylor, P.B., Kenno, K.A., 1992. Myocardial stretch alters twitch characteristics and Ca^{2+} loading of sarcoplasmic reticulum in rat ventricular muscle. Cardiovasc Res. 26, 865–870.
Gaskell, W.H., 1882. The Croonian Lecture. On the rhythm of the heart of the frog, and on the nature of the action of the vagus nerve. Philos. Trans. R. Soc. Lond 173, 993–1033.
Genge, C.E., Lin, E., Lee, L., Sheng, X., Rayani, K., Gunawan, M., Stevens, C.M., Li, A.Y., Talab, S.S., Claydon, T.W., Hove-Madsen, L., Tibbits, G.F., 2016. The zebrafish heart as a model of mammalian cardiac function. Rev. Physiol. Biochem. Pharmacol. 171, 99–136.
Gordan, R., Gwathmey, J.K., Xie, L.H., 2015. Autonomic and endocrine control of cardiovascular function. World J. Cardiol. 7, 204–214.
Guharay, F., Sachs, F., 1984. Stretch-activated single ion channel currents in tissue-cultured embryonic chick skeletal muscle. J. Physiol. 352, 685–701.
Gut, P., Reischauer, S., Stainier, D.Y.R., Arnaout, R., 2017. Little fish, big data: zebrafish as a model for cardiovascular and metabolic disease. Physiol. Rev. 97, 889–938.
Han, S., Wilson, S.J., Bolter, C.P., 2010. Tertiapin-Q removes a mechanosensitive component of muscarinic control of the sinoatrial pacemaker in the rat. Clin. Exp. Pharmacol. Physiol. 37, 900–904.
Hansen, D.E., Craig, C.S., Hondeghem, L.M., 1990. Stretch-induced arrhythmias in the isolated canine ventricle. Evidence for the importance of mechanoelectrical feedback. Circulation 81, 1094–1105.
Haustein, M., Hannes, T., Trieschmann, J., Verhaegh, R., Koster, A., Hescheler, J., Brockmeier, K., Adelmann, R., Khalil, M., 2015. Excitation-contraction coupling in zebrafish ventricular myocardium is regulated by trans-sarcolemmal Ca2+ influx and sarcoplasmic reticulum Ca2+ release. PLoS One 10, e0125654.
Hodgson-Zingman, D.M., Karst, M.L., Zingman, L.V., Heublein, D.M., Darbar, D., Herron, K.J., Ballew, J.D., de Andrade, M., Burnett Jr., J.C., Olson, T.M., 2008. Atrial natriuretic peptide frameshift mutation in familial atrial fibrillation. N. Engl. J. Med. 359, 158–165.
Hoffman, B.F., Cranefield, P.F., 1960. Electrophysiology of the Heart, first ed. McGraw-Hill, New York.
Hoffmann, S., Berger, I.M., Glaser, A., Bacon, C., Li, L., Gretz, N., Steinbeisser, H., Rottbauer, W., Just, S., Rappold, G., 2013. Islet1 is a direct transcriptional target of the homeodomain transcription factor Shox2 and rescues the Shox2-mediated bradycardia. Basic Res. Cardiol. 108, 339.
Horner, S.M., Murphy, C.F., Coen, B., Dick, D.J., Harrison, F.G., Vespalcova, Z., Lab, M.J., 1996. Contribution to heart rate variability by mechanoelectric feedback. Stretch of the sinoatrial node reduces heart rate variability. Circulation 94, 1762–1767.
Howe, K., Clark, M.D., Torroja, C.F., Torrance, J., Berthelot, C., Muffato, M., Collins, J.E., Humphray, S., McLaren, K., Matthews, L., McLaren, S., Sealy, I., Caccamo, M., Churcher, C., Scott, C., Barrett, J.C., Koch, R., Rauch, G.J., White, S., Chow, W., Kilian, B., Quintais, L.T., Guerra-Assuncao, J.A., Zhou, Y., Gu, Y., Yen, J., Vogel, J.H., Eyre, T., Redmond, S., Banerjee, R., Chi, J., Fu, B., Langley, E., Maguire, S.F., Laird, G.K., Lloyd, D., Kenyon, E., Donaldson, S., Sehra, H., Almeida-King, J., Loveland, J., Trevanion, S., Jones, M., Quail, M., Willey, D., Hunt, A., Burton, J., Sims, S., McLay, K., Plumb, B., Davis, J., Clee, C., Oliver, K., Clark, R., Riddle, C., Elliot, D., Threadgold, G., Harden, G., Ware, D., Begum, S., Mortimore, B., Kerry, G., Heath, P., Phillimore, B., Tracey, A., Corby, N., Dunn, M., Johnson, C., Wood, J., Clark, S., Pelan, S., Griffiths, G., Smith, M., Glithero, R., Howden, P., Barker, N., Lloyd, C., Stevens, C., Harley, J., Holt, K., Panagiotidis, G., Lovell, J., Beasley, H., Henderson, C., Gordon, D., Auger, K., Wright, D., Collins, J., Raisen, C., Dyer, L., Leung, K., Robertson, L., Ambridge, K., Leongamornlert, D., McGuire, S., Gilderthorp, R., Griffiths, C., Manthravadi, D., Nichol, S., Barker, G., et al., 2013. The zebrafish reference genome sequence and its relationship to the human genome. Nature 496, 498–503.
Hu, N., Yost, H.J., Clark, E.B., 2001. Cardiac morphology and blood pressure in the adult zebrafish. Anat. Rec. 264, 1–12.
Hua, R., MacLeod, S.L., Polina, I., Moghtadaei, M., Jansen, H.J., Bogachev, O., O'Blenes, S.B., Sapp, J.L., Legare, J.F., Rose, R.A., 2015. Effects of wild-type and mutant forms of atrial natriuretic peptide on atrial electrophysiology and arrhythmogenesis. Circ. Arrhythm. Electrophysiol. 8, 1240–1254.
Iribe, G., Kohl, P., 2008. Axial stretch enhances sarcoplasmic reticulum Ca^{2+} leak and cellular Ca^{2+} reuptake in Guinea pig ventricular myocytes: experiments and models. Prog. Biophys. Mol. Biol. 97, 298–311.
Iribe, G., Ward, C.W., Camelliti, P., Bollensdorff, C., Mason, F., Burton, R.A., Garny, A., Morphew, M.K., Hoenger, A., Lederer, W.J., Kohl, P., 2009. Axial stretch of rat single ventricular cardiomyocytes causes an acute and transient increase in

Ca^{2+} spark rate. Circ. Res. 104, 787–795.
Irisawa, H., Brown, H.F., Giles, W., 1993. Cardiac pacemaking in the sinoatrial node. Physiol. Rev. 73, 197–227.
Ishikawa, T., Yanagisawa, M., Kimura, S., Goto, K., Masaki, T., 1988. Positive chronotropic effects of endothelin, a novel endothelium-derived vasoconstrictor peptide. Pflugers Arch. 413, 108–110.
Jackson, H.A., Marshall, C.R., Accili, E.A., 2007. Evolution and structural diversification of hyperpolarization-activated cyclic nucleotide-gated channel genes. Physiol. Genomics 29, 231–245.
Ju, Y.K., Liu, J., Lee, B.H., Lai, D., Woodcock, E.A., Lei, M., Cannell, M.B., Allen, D.G., 2011. Distribution and functional role of inositol 1,4,5-trisphosphate receptors in mouse sinoatrial node. Circ. Res. 109, 848–857.
Kamiyama, A., Niimura, I., Sugi, H., 1984. Length-dependent changes of pacemaker frequency in the isolated rabbit sinoatrial node. Jpn. J. Physiol. 34, 153–165.
Keith, A., Flack, M., 1907. The form and nature of the muscular connections between the primary divisions of the vertebrate heart. J. Anat. Physiol. 41, 172–189.
Kobayashi, M., Furukawa, Y., Chiba, S., 1978. Positive chronotropic and inotropic effects of angiotensin II in the dog heart. Eur. J. Pharmacol. 50, 17–25.
Kohl, P., Noble, D., 1996. Mechanosensitive connective tissue: potential influence on heart rhythm. Cardiovasc Res. 32, 62–68.
Kohl, P., Kamkin, A.G., Kiseleva, I.S., Noble, D., 1994. Mechanosensitive fibroblasts in the sino-atrial node region of rat heart: interaction with cardiomyocytes and possible role. Exp. Physiol. 79, 943–956.
Koizumi, K., Terui, N., Kollai, M., Brooks, C.M., 1982. Functional significance of coactivation of vagal and sympathetic cardiac nerves. Proc. Natl. Acad. Sci. U. S. A. 79, 2116–2120.
Kollai, M., Koizumi, K., 1979. Reciprocal and non-reciprocal action of the vagal and sympathetic nerves innervating the heart. J. Auton. Nerv. Syst. 1, 33–52.
Kottkamp, H., 2012. Fibrotic atrial cardiomyopathy: a specific disease/syndrome supplying substrates for atrial fibrillation, atrial tachycardia, sinus node disease, AV node disease, and thromboembolic complications. J. Cardiovasc Electrophysiol. 23, 797–799.
Kuhn, M., 2004. Molecular physiology of natriuretic peptide signalling. Basic Res. Cardiol. 99, 76–82.
Kumagai, K., Akimitsu, S., Kawahira, K., Kawanami, F., Yamanouchi, Y., Hiroki, T., Arakawa, K., 1991. Electrophysiological properties in chronic lone atrial fibrillation. Circulation 84, 1662–1668.
Lakatta, E.G., Vinogradova, T.M., Maltsev, V.A., 2008. The missing link in the mystery of normal automaticity of cardiac pacemaker cells. Ann. N. Y. Acad. Sci. 1123, 41–57.
Lakatta, E.G., Maltsev, V.A., Vinogradova, T.M., 2010. A coupled SYSTEM of intracellular Ca^{2+} clocks and surface membrane voltage clocks controls the timekeeping mechanism of the heart's pacemaker. Circ. Res. 106, 659–673.
Lambert, C., 1995. Mechanisms of angiotensin II chronotropic effect in anaesthetized dogs. Br. J. Pharmacol. 115, 795–800.
Lambert, C., Godin, D., Fortier, P., Nadeau, R., 1991. Direct effects in vivo of angiotensins I and II on the canine sinus node. Can. J. Physiol. Pharmacol. 69, 389–392.
Lange, G., Lu, H.H., Chang, A., Brooks, C.M., 1966. Effect of stretch on the isolated cat sinoatrial node. Am. J. Physiol. 211, 1192–1196.
Leger, J., Croll, R.P., Smith, F.M., 1999. Regional distribution and extrinsic innervation of intrinsic cardiac neurons in the Guinea pig. J. Comp. Neurol. 407, 303–317.
Lei, M., Zhang, H., Grace, A.A., Huang, C.L., 2007. SCN5A and sinoatrial node pacemaker function. Cardiovasc Res. 74, 356–365.
Lin, W., Laitko, U., Juranka, P.F., Morris, C.E., 2007. Dual stretch responses of mHCN2 pacemaker channels: accelerated activation, accelerated deactivation. Biophys. J. 92, 1559–1572.
Lin, E., Ribeiro, A., Ding, W., Hove-Madsen, L., Sarunic, M.V., Beg, M.F., Tibbits, G.F., 2014. Optical mapping of the electrical activity of isolated adult zebrafish hearts: acute effects of temperature. Am. J. Physiol. Regul. Integr. Comp. Physiol. 306, R823–R836.
Liu, C.C., Li, L., Lam, Y.W., Siu, C.W., Cheng, S.H., 2016. Improvement of surface ECG recording in adult zebrafish reveals that the value of this model exceeds our expectation. Sci. Rep. 6, 25073.
Llach, A., Molina, C.E., Alvarez-Lacalle, E., Tort, L., Benitez, R., Hove-Madsen, L., 2011. Detection, properties, and frequency of local calcium release from the sarcoplasmic reticulum in teleost cardiomyocytes. PLoS One 6, e23708.
Lonardo, G., Cerbai, E., Casini, S., Giunti, G., Bonacchi, M., Battaglia, F., Fiorani, B., Stefano, P.L., Sani, G., Mugelli, A., 2004. Atrial natriuretic peptide modulates the hyperpolarization-activated current (If) in human atrial myocytes. Cardiovasc Res. 63, 528–536.
Lucas, K.A., Pitari, G.M., Kazerounian, S., Ruiz-Stewart, I., Park, J., Schulz, S., Chepenik, K.P., Waldman, S.A., 2000. Guanylyl cyclases and signaling by cyclic GMP. Pharmacol. Rev. 52, 375–414.
Lyford, G.L., Strege, P.R., Shepard, A., Ou, Y., Ermilov, L., Miller, S.M., Gibbons, S.J., Rae, J.L., Szurszewski, J.H., Farrugia, G., 2002. α_{1C} ($Ca_V1.2$) L-type calcium channel mediates mechanosensitive calcium regulation. Am. J. Physiol. Cell Physiol. 283, C1001–C1008.
Maltsev, V.A., Lakatta, E.G., 2012. The funny current in the context of the coupled-clock pacemaker cell system. Heart Rhythm 9, 302–307.
Maltsev, V.A., Vinogradova, T.M., Lakatta, E.G., 2006. The emergence of a general theory of the initiation and strength of the heartbeat. J. Pharmacol. Sci. 100, 338–369.
Marshall, C.R., Fox, J.A., Butland, S.L., Ouellette, B.F., Brinkman, F.S., Tibbits, G.F., 2005. Phylogeny of Na+/Ca2+ exchanger (NCX) genes from genomic data identifies new gene duplications and a new family member in fish species. Physiol. Genomics 21, 161–173.
McGowan, C.L., Swiston, J.S., Notarius, C.F., Mak, S., Morris, B.L., Picton, P.E., Granton, J.T., Floras, J.S., 2009. Discordance between microneurographic and heart-rate spectral indices of sympathetic activity in pulmonary arterial hypertension. Heart 95, 754–758.
Mesirca, P., Torrente, A.G., Mangoni, M.E., 2015. Functional role of voltage gated Ca(2+) channels in heart automaticity. Front. Physiol. 6, 19.
Moghtadaei, M., Polina, I., Rose, R.A., 2016. Electrophysiological effects of natriuretic peptides in the heart are mediated by multiple receptor subtypes. Prog. Biophys. Mol. Biol. 120, 37–49.
Mohler, P.J., Anderson, M.E., 2008. New insights into genetic causes of sinus node disease and atrial fibrillation. J. Cardiovasc Electrophysiol. 19, 516–518.
Monfredi, O., Dobrzynski, H., Mondal, T., Boyett, M.R., Morris, G.M., 2010. The anatomy and physiology of the sinoatrial node–a contemporary review. Pacing Clin. Electrophysiol. 33, 1392–1406.
Morris, C.E., 2011. Pacemaker, potassium, calcium, sodium: stretch modulation of the volatge-gated channels. In: Kohl, P., Sachs, F., Franz, M.R. (Eds.), Cardiac Mechano-electric Coupling and Arrhythmias. Oxford University Press, Oxford, pp. 42–49.
Morton, J.B., Sanders, P., Vohra, J.K., Sparks, P.B., Morgan, J.G., Spence, S.J., Grigg, L.E., Kalman, J.M., 2003. Effect of chronic right atrial stretch on atrial electrical remodeling in patients with an atrial septal defect. Circulation 107, 1775–1782.
Muszkiewicz, A., Britton, O.J., Gemmell, P., Passini, E., Sanchez, C., Zhou, X., Carusi, A., Quinn, T.A., Burrage, K., Bueno-Orovio, A., Rodriguez, B., 2016. Variability in cardiac electrophysiology: using experimentally-calibrated populations of models to move beyond the single virtual physiological human paradigm. Prog. Biophys. Mol. Biol. 120, 115–127.
Nakao, S., Hirakawa, A., Fukushima, R., Kobayashi, M., Machida, N., 2012. The anatomical basis of bradycardia-tachycardia syndrome in elderly dogs with chronic degenerative valvular disease. J. Comp. Pathol. 146, 175–182.
Nemtsas, P., Wettwer, E., Christ, T., Weidinger, G., Ravens, U., 2010. Adult zebrafish heart as a model for human heart? An electrophysiological study. J. Mol. Cell Cardiol. 48, 161–171.
Nilsson, S., 1983. Autonomic Nerve Function in the Vertebrates. Springer-Verlag, Berlin.
Nilsson, S., Holmgren, S., 1994. Comparative Physiology and Evolution of the Autonomic Nervous System. Harwood Academic Publishers, Chur, Switzerland.
Nishimura, S., Seo, K., Nagasaki, M., Hosoya, Y., Yamashita, H., Fujita, H., Nagai, R., Sugiura, S., 2008. Responses of single-ventricular myocytes to dynamic axial stretching. Prog. Biophys. Mol. Biol. 97, 282–297.
Ono, K., Masumiya, H., Sakamoto, A., Christe, G., Shijuku, T., Tanaka, H., Shigenobu, K., Ozaki, Y., 2001. Electrophysiological analysis of the negative chronotropic effect of endothelin-1 in rabbit sinoatrial node cells. J. Physiol. 537, 467–488.
Pardini, B.J., Patel, K.P., Schmid, P.G., Lund, D.D., 1987. Location, distribution and projections of intracardiac ganglion cells in the rat. J. Auton. Nerv. Syst. 20, 91–101.
Pathak, C.L., 1973. Autoregulation of chronotropic response of the heart through pacemaker stretch. Cardiology 58, 45–64.
Pauza, D.H., Skripka, V., Pauziene, N., Stropus, R., 2000. Morphology, distribution, and variability of the epicardiac neural ganglionated subplexuses in the human heart. Anat. Rec. 259, 353–382.
Perrin, M.J., Gollob, M.H., 2012. The role of atrial natriuretic peptide in modulating cardiac electrophysiology. Heart Rhythm 9, 610–615.
Peyronnet, R., Nerbonne, J.M., Kohl, P., 2016. Cardiac mechano-gated ion channels and arrhythmias. Circ. Res. 118, 311–329.
Poon, K.L., Brand, T., 2013. The zebrafish model system in cardiovascular research: a tiny fish with mighty prospects. Glob. Cardiol. Sci. Pract. 2013, 9–28.
Poon, K.L., Liebling, M., Kondrychyn, I., Brand, T., Korzh, V., 2016. Development of the cardiac conduction system in zebrafish. Gene Expr. Patterns 21, 89–96.
Potter, L.R., Abbey-Hosch, S., Dickey, D.M., 2006. Natriuretic peptides, their receptors, and cyclic guanosine monophosphate-dependent signaling functions. Endocr. Rev. 27, 47–72.
Prosser, B.L., Ward, C.W., Lederer, W.J., 2011. X-ROS signaling: rapid mechano-chemo transduction in heart. Science 333, 1440–1445.
Prosser, B.L., Ward, C.W., Lederer, W.J., 2013. X-ROS signalling is enhanced and graded by cyclic cardiomyocyte stretch. Cardiovasc Res. 98, 307–314.
Quinn, T.A., 2014. The importance of non-uniformities in mechano-electric coupling for ventricular arrhythmias. J. Interv. Card. Electrophysiol. 39, 25–35.
Quinn, T.A., 2015. Cardiac mechano-electric coupling: a role in regulating normal function of the heart? Cardiovasc Res. 108, 1–3.
Quinn, T.A., Kohl, P., 2011a. Mechanical triggers and facilitators of ventricular tachyarrhythmias. In: Kohl, P., Sachs, F., Franz, M.R. (Eds.), Cardiac Mechano-electric Coupling and Arrhythmias. Oxford University Press, Oxford, pp. 160–167.
Quinn, T.A., Kohl, P., 2011b. Systems biology of the heart: hype or hope? Ann. N. Y. Acad. Sci. 1245, 40–43.
Quinn, T.A., Kohl, P., 2012. Mechano-sensitivity of cardiac pacemaker function: pathophysiological relevance, experimental implications, and conceptual integration with other mechanisms of rhythmicity. Prog. Biophys. Mol. Biol. 110, 257–268.
Quinn, T.A., Kohl, P., 2013. Combining wet and dry research: experience with model development for cardiac mechano-electric structure-function studies. Cardiovasc Res. 97, 601–611.
Quinn, T.A., Kohl, P., 2016. Rabbit models of cardiac mechano-electric and mechano-

mechanical coupling. Prog. Biophys. Mol. Biol. 121, 110–122.
Quinn, T.A., Bayliss, R.A., Kohl, P., 2011a. Mechano-electric feedback in the heart: effects on heart rate and rhythm. In: Tripathi, O.N., Ravens, U., Sanguinetti, M.C. (Eds.), Heart Rate and Rhythm: Molecular Basis, Pharmacological Modulation and Clinical Implications. Springer, Heidelberg, pp. 133–151.
Quinn, T.A., Granite, S., Allessie, M.A., Antzelevitch, C., Bollensdorff, C., Bub, G., Burton, R.A., Cerbai, E., Chen, P.S., Delmar, M., Difrancesco, D., Earm, Y.E., Efimov, I.R., Egger, M., Entcheva, E., Fink, M., Fischmeister, R., Franz, M.R., Garny, A., Giles, W.R., Hannes, T., Harding, S.E., Hunter, P.J., Iribe, G., Jalife, J., Johnson, C.R., Kass, R.S., Kodama, I., Koren, G., Lord, P., Markhasin, V.S., Matsuoka, S., McCulloch, A.D., Mirams, G.R., Morley, G.E., Nattel, S., Noble, D., Olesen, S.P., Panfilov, A.V., Trayanova, N.A., Ravens, U., Richard, S., Rosenbaum, D.S., Rudy, Y., Sachs, F., Sachse, F.B., Saint, D.A., Schotten, U., Solovyova, O., Taggart, P., Tung, L., Varro, A., Volders, P.G., Wang, K., Weiss, J.N., Wettwer, E., White, E., Wilders, R., Winslow, R.L., Kohl, P., 2011b. Minimum Information about a Cardiac Electrophysiology Experiment (MICEE): standardised reporting for model reproducibility, interoperability, and data sharing. Prog. Biophys. Mol. Biol. 107, 4–10.
Quinn, T.A., Kohl, P., Ravens, U., 2014. Cardiac mechano-electric coupling research: fifty years of progress and scientific innovation. Prog. Biophys. Mol. Biol. 115, 71–75.
Quinn, T.A., Camelliti, P., Rog-Zielinska, E.A., Siedlecka, U., Poggioli, T., O'Toole, E.T., Knopfel, T., Kohl, P., 2016. Electrotonic coupling of excitable and nonexcitable cells in the heart revealed by optogenetics. Proc. Natl. Acad. Sci. U. S. A. 113, 14852–14857.
Rajala, G.M., Pinter, M.J., Kaplan, S., 1977. Response of the quiescent heart tube to mechanical stretch in the intact chick embryo. Dev. Biol. 61, 330–337.
Rajendran, P.S., Nakamura, K., Ajijola, O.A., Vaseghi, M., Armour, J.A., Ardell, J.L., Shivkumar, K., 2016. Myocardial infarction induces structural and functional remodelling of the intrinsic cardiac nervous system. J. Physiol. 594, 321–341.
Rose, R.A., Giles, W.R., 2008. Natriuretic peptide C receptor signalling in the heart and vasculature. J. Physiol. 586, 353–366.
Rose, R.A., Lomax, A.E., Kondo, C.S., Anand-Srivastava, M.B., Giles, W.R., 2004. Effects of C-type natriuretic peptide on ionic currents in mouse sinoatrial node: a role for the NPR-C receptor. Am. J. Physiol. Heart Circ. Physiol. 286, H1970–H1977.
Rose, R.A., Hatano, N., Ohya, S., Imaizumi, Y., Giles, W.R., 2007. C-type natriuretic peptide activates a non-selective cation current in acutely isolated rat cardiac fibroblasts via natriuretic peptide C receptor-mediated signalling. J. Physiol. 580, 255–274.
Rosen, M.R., Nargeot, J., Salama, G., 2012. The case for the funny current and the calcium clock. Heart Rhythm 9, 616–618.
Rubenstein, J.J., Schulman, C.L., Yurchak, P.M., DeSanctis, R.W., 1972. Clinical spectrum of the sick sinus syndrome. Circulation 46, 5–13.
Saito, K., Gutkind, J.S., Saavedra, J.M., 1987. Angiotensin II binding sites in the conduction system of rat hearts. Am. J. Physiol. 253, H1618–H1622.
Sanders, R., Myerburg, R.J., Gelband, H., Bassett, A.L., 1979. Dissimilar length–tension relations of canine ventricular muscle and false tendon: electrophysiologic alterations accompanying deformation. J. Mol. Cell Cardiol. 11, 209–219.
Sanders, P., Morton, J.B., Davidson, N.C., Spence, S.J., Vohra, J.K., Sparks, P.B., Kalman, J.M., 2003. Electrical remodeling of the atria in congestive heart failure: electrophysiological and electroanatomic mapping in humans. Circulation 108, 1461–1468.
Schindler, R.F., Poon, K.L., Simrick, S., Brand, T., 2012. The Popeye domain containing genes: essential elements in heart rate control. Cardiovasc Diagn Ther. 2, 308–319.
Schwerte, T., Prem, C., Mairosl, A., Pelster, B., 2006. Development of the sympathovagal balance in the cardiovascular system in zebrafish (Danio rerio) characterized by power spectrum and classical signal analysis. J. Exp. Biol. 209, 1093–1100.
Sheng, J.W., Wang, W.Y., Xu, Y.F., 2011. Angiotensin II decreases spontaneous firing rate of Guinea-pig sino-atrial node cells. Eur. J. Pharmacol. 660, 387–393.
Sidi, S., Busch-Nentwich, E., Friedrich, R., Schoenberger, U., Nicolson, T., 2004. Gemini encodes a zebrafish L-type calcium channel that localizes at sensory hair cell ribbon synapses. J. Neurosci. 24, 4213–4223.
Smith, F.M., 1999. Extrinsic inputs to intrinsic neurons in the porcine heart in vitro. Am. J. Physiol. 276, R455–R467.
Smith, F.M., McGuirt, A.S., Leger, J., Armour, J.A., Ardell, J.L., 2001. Effects of chronic cardiac decentralization on functional properties of canine intracardiac neurons in vitro. Am. J. Physiol. Regul. Integr. Comp. Physiol. 281, R1474–R1482.
Sparks, P.B., Mond, H.G., Vohra, J.K., Jayaprakash, S., Kalman, J.M., 1999. Electrical remodeling of the atria following loss of atrioventricular synchrony: a long-term study in humans. Circulation 100, 1894–1900.
Springer, J., Azer, J., Hua, R., Robbins, C., Adamczyk, A., McBoyle, S., Bissell, M.B., Rose, R.A., 2012. The natriuretic peptides BNP and CNP increase heart rate and electrical conduction by stimulating ionic currents in the sinoatrial node and atrial myocardium following activation of guanylyl cyclase-linked natriuretic peptide receptors. J. Mol. Cell Cardiol. 52, 1122–1134.
Steele, P.A., Choate, J.K., 1994. Innervation of the pacemaker in Guinea-pig sinoatrial node. J. Auton. Nerv. Syst. 47, 177–187.
Steele, P.A., Gibbins, I.L., Morris, J.L., 1996. Projections of intrinsic cardiac neurons to different targets in the Guinea-pig heart. J. Auton. Nerv. Syst. 56, 191–200.
Stockbridge, L.L., French, A.S., 1988. Stretch-activated cation channels in human fibroblasts. Biophys. J. 54, 187–190.
Stoyek, M.R., Croll, R.P., Smith, F.M., 2015. Intrinsic and extrinsic innervation of the heart in zebrafish (Danio rerio). J. Comp. Neurol. 523, 1683–1700.
Stoyek, M.R., Quinn, T.A., Croll, R.P., Smith, F.M., 2016. Zebrafish heart as a model to study the integrative autonomic control of pacemaker function. Am. J. Physiol. Heart Circ. Physiol. 311, H676–H688.
Tanaka, H., Habuchi, Y., Yamamoto, T., Nishio, M., Morikawa, J., Yoshimura, M., 1997. Negative chronotropic actions of endothelin-1 on rabbit sinoatrial node pacemaker cells. Br. J. Pharmacol. 122, 321–329.
Task Force of the European Society of Cardiology and the North American Society of Pacing and Electrophysiology, 1996. Heart rate variability: standards of measurement, physiological interpretation and clinical use. Circulation 93, 1043–1065.
Tessadori, F., van Weerd, J.H., Burkhard, S.B., Verkerk, A.O., de Pater, E., Boukens, B.J., Vink, A., Christoffels, V.M., Bakkers, J., 2012. Identification and functional characterization of cardiac pacemaker cells in zebrafish. PLoS One 7, e47644.
Torrente, A.G., Mesirca, P., Neco, P., Rizzetto, R., Dubel, S., Barrere, C., Sinegger-Brauns, M., Striessnig, J., Richard, S., Nargeot, J., Gomez, A.M., Mangoni, M.E., 2016. L-type Cav1.3 channels regulate ryanodine receptor-dependent Ca2+ release during sino-atrial node pacemaker activity. Cardiovasc Res. 109, 451–461.
Tota, B., Amelio, D., Pellegrino, D., Ip, Y.K., Cerra, M.C., 2005. No modulation of myocardial performance in fish hearts. Comp. Biochem. Physiol. A Mol. Integr. Physiol. 142, 164–177.
Vornanen, M., Hassinen, M., 2016. Zebrafish heart as a model for human cardiac electrophysiology. Channels (Austin) 10, 101–110.
Warren, K.S., Baker, K., Fishman, M.C., 2001. The slow mo mutation reduces pacemaker current and heart rate in adult zebrafish. Am. J. Physiol. Heart Circ. Physiol. 281, H1711–H1719.
Werdich, A.A., Brzezinski, A., Jeyaraj, D., Khaled Sabeh, M., Ficker, E., Wan, X., McDermott Jr., B.M., Macrae, C.A., Rosenbaum, D.S., 2012. The zebrafish as a novel animal model to study the molecular mechanisms of mechano-electrical feedback in the heart. Prog. Biophys. Mol. Biol. 110, 154–165.
Wilson, S.J., Bolter, C.P., 2001. Interaction of the autonomic nervous system with intrinsic cardiac rate regulation in the Guinea-pig, Cavia porcellus. Comp. Biochem. Physiol. A Mol. Integr. Physiol. 130, 723–730.
Wilson, S.J., Bolter, C.P., 2002. Do cardiac neurons play a role in the intrinsic control of heart rate in the rat? Exp. Physiol. 87, 675–682.
Yaniv, Y., Spurgeon, H.A., Lyashkov, A.E., Yang, D., Ziman, B.D., Maltsev, V.A., Lakatta, E.G., 2012. Crosstalk between mitochondrial and sarcoplasmic reticulum Ca^{2+} cycling modulates cardiac pacemaker cell automaticity. PLoS One 7, e37582.
Yuan, B.X., Ardell, J.L., Hopkins, D.A., Losier, A.M., Armour, J.A., 1994. Gross and microscopic anatomy of the canine intrinsic cardiac nervous system. Anat. Rec. 239, 75–87.
Zhang, P.C., Llach, A., Sheng, X.Y., Hove-Madsen, L., Tibbits, G.F., 2011. Calcium handling in zebrafish ventricular myocytes. Am. J. Physiol. Regul. Integr. Comp. Physiol. 300, R56–R66.